Role of Protons in the Thermodynamic Contribution of a Zn(II)-Cys_4 Site toward Metalloprotein Stability†

Amit R. Reddi and Brian R. Gibney*

Department of Chemistry, Columbia University, 3000 Broadway MC 3121, New York, New York 10027

Received October 31, 2006; Revised Manuscript Received January 22, 2007

ABSTRACT: The current limited understanding of the free energy contributions of metal−protein interactions toward metalloprotein stability is largely due to an inability to separate the energetics of the metal−ligand and protein−protein interactions. In order to elucidate the thermodynamic contribution of a Zn(II)−$(S{\cdot}Cys)_4$ site toward metalloprotein stability relevant to classic structural Zn(II) sites, the reaction of $\{Zn(II)(H_2O)_6\}^{2+}$ with a minimal, unstructured, tetracysteine 16-mer peptide, **GGG**, is described. Isothermal titration fluorimetry over the pH range of 4.5 to 9.0 is used to measure the free energy of Zn(II) binding to the model peptide **GGG**. The data show that, in the absence of proton competition, Zn(II) binds to the Cys_4 coordination sphere with a K_d of 60 aM, indicating that the Zn(II)−$(S{\cdot}Cys)_4$ interaction can provide up to 22.1 kcal mol^{-1} in driving force for protein stabilization, folding, and/or assembly. Isothermal titration calorimetry shows that Zn(II)−**GGG** formation is entropy driven because of water release from both the metal and the peptide scaffold. At pH 7.0, where the Zn(II)−**GGG** K_d value is 8.0 pM, the reaction releases 3.8 protons, is endothermic with ΔH_{rxn} of +6.4 kcal mol^{-1}, and entropy driven with ΔS_{rxn} of +72 cal K^{-1} mol^{-1}. At pH 8.0, where the peptide is partially deprotonated prior to Zn(II) binding, the 1.0 fM Zn(II)−**GGG** K_d value reflects a Zn(II) complexation reaction involving the release of 2.5 protons, which is slightly exothermic, with ΔH_{rxn} of −2.0 kcal mol^{-1}, and largely entropy driven, with ΔS_{rxn} of +61 cal K^{-1} mol^{-1}. At pH 5.5, where proton competition weakens the K_d to 4.0 μM, only 3.2 protons are released upon Zn(II) binding, the reaction is endothermic, with ΔH_{rxn} of +7.7 kcal mol^{-1}, and entropy driven, with ΔS_{rxn} of +51 cal K^{-1} mol^{-1}. Likely an intrinsic property of Zn(II)−$(S{\cdot}Cys)_4$ sites, the entropy driven binding of Zn(II) reflects the proton dependent chemical speciation of the Zn(II)−$(S{\cdot}Cys)_4$ peptide complex and its effects on modulating the dehydration of both the peptide and metal. Furthermore, the Zn(II) binding thermodynamics of a variety of Zn(II) proteins at pH 7.0 reveals the presence of enthalpy−entropy compensation (EEC) phenomena in nature.

Nature utilizes a variety of cofactors and prosthetic groups to augment protein structure and function. Zn(II) is one of the most pervasive metal cofactors in biology, serving proteins in both catalytic and structural capacities (*1*). Of the 2800 Zn(II)-binding proteins in humans, corresponding to 10% of the proteome, one-third fully coordinate the metal using four cysteine ligands (*2*); thus, the Zn(II)−$(S{\cdot}Cys)_4$ moiety is an essential and ubiquitous cofactor−protein interaction. The majority of natural Zn(II)−$(S{\cdot}Cys)_4$ sites are structural, endowing proteins with the ability to fold into their unique tertiary structures required for proper biological function. Despite the importance of the Zn(II)−$(S{\cdot}Cys)_4$ unit in stabilizing protein structure, there is a limited understanding of the free energy contributions of the Zn(II)−$(S{\cdot}Cys)_4$ site toward metalloprotein structure, folding, and function. This is largely due to the inability to separate the energetics of the metal−ligand interactions from the sea of protein−protein interactions present, for example, hydrogen bonds and electrostatic interactions. This is especially true in cases where Zn(II) coordination is coupled to protein folding, for example, the zinc finger transcription factors (*1*, *3*, *4*). Delineating the thermodynamics of Zn(II) coordination to a Cys_4 site is further complicated by the pH sensitivity because the conditional dissociation constant value, K_d, possesses a $[H^+]^4$ dependence due to the release of one proton per cysteine thiol upon coordination. This $[H^+]^4$ dependence translates into a 10,000-fold, or 5.5 kcal mol^{-1}, change in binding affinity per pH unit in between the pK_a[1] values of the uncomplexed cysteine and the Zn(II)-bound cysteine thiol.

† This work was supported by an American Heart Association grant to B.R.G. (0455900T). A.R.R. acknowledges receipt of a National Science Foundation GK-12 Fellowship (DGE-02-31875).

* Corresponding author. Phone: (212) 854-6346. Fax: (212) 932-1289. E-mail: brg@chem.columbia.edu.

[1] Abbreviations: TFA, trifluoroacetic acid; ESI/MS, electrospray ionization mass spectrometry; Fmoc, 9-fluorenylmethoxycarbonyl; ^{t}-Boc, *t*-butoxycarbonyl; PAL-PEG-PS, peptide amide linker-polyethylene glycol-polystyrene; HBTU, *O*-(1*H*-benzotriazole-1-yl)-*N*,*N*,*N*′,*N*′-tetramethyluronium hexafluorophosphate; O^{t}Bu, *tert*-butyl ester; Trt, trityl; HPLC, high-performance liquid chromatography; ITC, isothermal titration calorimetry; EDTA, ethylenediaminetetraacetic acid; EEC, enthalpy−entropy compensation; **GGG**, NH_2-KLCEGGCGGCGGCG-GW-$CONH_2$; PIPES, piperazine-1,4-bis(2-ethanesulfonic acid); HEPES, *N*-(2-hydroxyethyl)-piperazine-*N*′-2-ethanesulfonic acid; MES, 2-(*N*-morpholino)-ethanesulfonic acid; MOPS, 3-(*N*-morpholino)-propanesulfonic acid; pK_a, the negative logarithm of the acid dissociation constant of unbound cysteines in **GGG**; pK_a^{eff}, the negative logarithm of the acid dissociation constant of the metal-bound cysteines in the Zn(II)−**GGG** complex.

10.1021/bi062253w CCC: $37.00
Published on Web 02/28/2007

De novo protein design provides a constructive methodology for elucidating the structure−function relationships intrinsic to natural proteins (*5*). Advances in the design of stable, well-structured protein scaffolds are accelerating because of improvements in both minimization algorithms and energy functions based on the experimentally derived thermodynamic contributions of individual protein−protein interactions (*6*−*11*). Because inorganic cofactor−protein interactions are critical to metalloprotein structure, folding, and function, the current limited understanding of metal−protein interaction thermodynamics is restricting the parallel advancement of *de novo* metalloprotein design (*12*−*14*). In order to elucidate the fundamental metal−ligand binding thermodynamics, we are utilizing maquettes (*15*), simplified metallopeptides and metalloproteins, to delineate the free energy contributions of metal−protein interactions (*16*−*27*). We have designed a 16 amino acid peptide containing four cysteine residues, **IGA**, as a synthetic ferredoxin and have used this scaffold to evaluate the selectivity of a tetrahedral tetrathiolate site for Fe(II), Co(II), Zn(II), and a $[4Fe\text{-}4S]^{2+}$ cluster (*17*−*21*). By analyzing the coupled metal−ligand and proton−ligand equilibria, we have elucidated the pH independent dissociation constants of Fe(II)-**IGA**, Co(II)-**IGA**, and Zn(II)−**IGA**, which are 2.0 nM, 2.0 pM, and 125 aM, respectively (*21*). These thermodynamic studies provide the data necessary for improving the energy functions for computational metalloprotein design as well as deconvoluting the energetics of metal−protein assemblies in nature, that is, parsing apart the free energy contributions to metalloprotein stability into its constituent thermodynamic components (*26*, *28*−*36*).

Herein, we utilize **GGG**, a variant of **IGA** having the primary structure NH_2-KLCEGG·C**GG**CG**G**C·GGW-$CONH_2$, to elucidate the role of protons in the thermodynamic contribution of a Zn(II)−$(S{\cdot}Cys)_4$ site toward metalloprotein stability relevant to structural Zn(II)−$(S{\cdot}Cys)_4$ sites. Because the sequence of **IGA** was originally derived from the clostridial [4Fe-4S] binding motif (*18*, *21*), **GGG** was designed to more closely emulate structural Zn(II) sites such as those found in zinc finger transcription factors, alcohol dehydrogenase, and cytochrome *c* oxidase (*1*). Using a combination of conditional dissociation constant measurements, EDTA competition constant measurements, and potentiometric pH titrations, we determine the pH independent dissociation constant for the Zn(II)−**GGG** complex to be 60 aM, which indicates that a Zn(II)−$(S{\cdot}Cys)_4$ site can provide up to 22.1 kcal mol^{-1} in driving force for protein stabilization, folding, and/or assembly. Isothermal titration calorimetry further shows that a majority of this driving force is entropic in origin and due to the dehydration of the metal and the *apo*-peptide upon metal binding, which is modulated by the pH dependent speciation of the Zn(II)−$(S{\cdot}Cys)_4$ complex and the free ligand, **GGG**. These experimental results, derived from a peptide with minimal protein folding effects, are used to reveal the energetic cost of protein folding in natural Zn(II)−$(S{\cdot}Cys)_4$ metalloproteins, heretofore unknown values in systems where protein folding is coupled to metal binding.

MATERIALS AND METHODS

Materials. Trifluoroacetic acid, ethanedithiol, 1-hydroxybenzotriazole, diethyl ether, acetic anhydride, diisopropylethylamine (DIEA), piperidine, and zinc(II)chloride were obtained from the Sigma-Aldrich Chemical Co. Aqueous stock solutions of Zn(II) were quantified by calorimetric EDTA titrations. Natural Fmoc-protected amino acids were obtained from Bachem. HBTU, *O*-(1*H*-benzotriazole-1-yl)-*N*,*N*,*N*′,*N*′-tetramethyluronium hexafluorophosphate, was purchased from Qbiogene. All other chemicals and solvents were reagent grade and used without further purification.

Chemical Synthesis of the Peptide. The peptide ligand **GGG** was synthesized using solid phase peptide synthesis (*37*) in a fashion analogous to that reported for the **IGA** peptide ligand (*21*).

UV−*Vis Spectroscopy*. UV−visible spectra were recorded on either a Varian Cary 100 or a Bio50 spectrophotometer using quartz cells of 1.0 cm path length. Peptide concentrations were determined spectrophotometrically using ϵ_{280} of 5600 M^{-1} cm^{-1} for Trp.

Fluorescence Spectroscopy. Excitation and emission fluorescence spectra were recorded on a Cary Eclipse fluorimeter using rectangular quartz cells of 1.0 cm path length. Excitation and emission slit widths of 5 nm were employed. pH titrations were performed using an automated titrator attached to an AVIV 215 circular dichroism spectropolarimeter with a total fluorescence attachment. The excitation wavelength was 280 nm, and the total fluorescence emission was collected after a 310 nm high band-pass filter. The sample was maintained at 25 °C by a thermoelectric module with a ThermoNeslab refrigerated recirculating water bath as a heat sink. Peptide concentrations were between 10 and 30 μM as determined spectrophotometrically using ϵ_{280} = 5600 M^{-1} cm^{-1} for Trp.

Isothermal Titration Fluorimetry: Direct Zn(II) Titrations. Aqueous stock solutions of $Zn(II)Cl_2$ unbuffered at pH 7.0 were added in microliter aliquots to freshly prepared **GGG** peptide solutions in aqueous buffers (20 mM MES and 100 mM KCl) under strictly anaerobic conditions in 1.0 cm cuvettes. Samples were allowed to equilibrate for 3 min before measuring their fluorescence spectra. The conditional metal−ligand dissociation constants, conditional K_d values, were obtained from fitting a plot of the increase in tryptophan fluorescence at 357 nm against the [Zn(II)]/[**GGG**] ratio to the following 1:1 equilibrium binding model.

$$\mathbf{GGG} + \{Zn(II)(H_2O)_6\}^{2+} \rightleftharpoons Zn(II)\text{−}\mathbf{GGG} + 6H_2O \quad (1)$$

$$K_d = \frac{[\{Zn(II)(H_2O)_6\}^{2+}][\mathbf{GGG}]}{[Zn(II) - \mathbf{GGG}]} \quad (2)$$

The equation used to fit the data is, as follows:

$$Fl_{meas} = Fl_0 + \frac{Fl_{lim} - Fl_0}{2L_T}[(M_T + L_T + K_d) - \sqrt{(-M_T - L_T - K_d)^2 - (4L_TM_T)}] \quad (3)$$

where Fl_{meas}, the measured fluorescence emission intensity, is a function of Fl_0, the fluorescence intensity of the **GGG** ligand prior to metal binding, Fl_{lim} is the limiting emission intensity of the Zn(II)−**GGG** complex, M_T is the total concentration of metal added to peptide solution, L_T is the total concentration of the **GGG** ligand, and K_d is the conditional dissociation constant.

Isothermal Titration Fluorimetry: EDTA Competition Titrations. For pH values above 6.0, conditional equilibrium dissociation constant determination for the Zn(II)−**GGG** complex necessitated the use of EDTA (ethylenediaminetetraacetic acid) competition. To buffered aqueous solutions (20 mM HEPES and 100 mM KCl) of 10−15 μM **GGG** and between 1.0 and 10 equiv of EDTA, an unbuffered aqueous solution of $Zn(II)Cl_2$ at pH 7.0 was added in microliter aliquots under strictly anaerobic conditions. The increase in fluorescence at 357 nm upon the addition of Zn(II) was fit to a competition equilibrium binding model based on eqs 4−8

$$\text{EDTA} + \{\text{Zn(II)(H}_2\text{O)}_6\}^{2+} \rightleftharpoons \text{Zn(II)-EDTA} + 6\text{H}_2\text{O} \quad (4)$$

$$\textbf{GGG} + \{\text{Zn(II)(H}_2\text{O)}_6\}^{2+} \rightleftharpoons \text{Zn(II)}-\textbf{GGG} + 6\text{H}_2\text{O} \quad (5)$$

$$K_{\text{comp}} = \frac{K_{\text{d}}^{\text{Zn(II)}-\text{EDTA}}}{K_{\text{d}}^{\text{Zn(II)}-\textbf{GGG}}} = \frac{[\text{EDTA}][\text{Zn(II)} - \textbf{GGG}]}{[\text{Zn(II)} - \text{EDTA}][\textbf{GGG}]} \quad (6)$$

$$Fl_{\text{meas}} = Fl_0 + \frac{Fl_{\text{lim}} - Fl_0}{2L_{\text{T}}(1 - K_{\text{comp}})}[\beta + \sqrt{\beta^2 + 4(1 - K_{\text{comp}})M_{\text{T}}L_{\text{T}}K_{\text{comp}}}] \quad (7)$$

$$\beta = M_{\text{T}} - \text{EDTA}_{\text{T}} - K_{\text{comp}}M_{\text{T}} - K_{\text{comp}}L_{\text{T}} \quad (8)$$

where Fl_{meas}, the measured fluorescence emission intensity, is a function of Fl_0, the fluorescence of the **GGG** ligand prior to metal binding, Fl_{lim}, the limiting fluorescence of the Zn(II)−**GGG** complex, M_{T}, the total concentration of metal added to the peptide solution, L_{T}, the total concentration of the **GGG** ligand, EDTA_{T}, the total concentration of EDTA, and K_{comp}, the conditional competition constant.

The K_{comp} value, coupled with the conditional equilibrium dissociation constant value of Zn(II)-EDTA, $K_{\text{d}}^{\text{Zn(II)}-\text{EDTA}}$, given by eqs 9−11, gives the conditional equilibrium dissociation constant value for Zn(II)−**GGG**.

$$K_{\text{d}}^{\text{Zn(II)}-\text{EDTA}} = \frac{1}{K_{\text{f}}^{\text{Zn(II)}-\text{EDTA}}\alpha_{\text{L}}} \quad (9)$$

$$\alpha_{\text{L}} = \frac{K_1K_2K_3K_4K_5K_6}{\text{EDTA}_{\text{T}}} \quad (10)$$

$$\text{EDTA}_{\text{T}} = K_1K_2K_3K_4K_5K_6 + K_1K_2K_3K_4K_5[\text{H}^+] + K_1K_2K_3K_4[\text{H}^+]^2 + K_1K_2K_3[\text{H}^+]^3 + K_1K_2[\text{H}^+]^4 + K_1[\text{H}^+]^5 + [\text{H}^+]^6 \quad (11)$$

α_{L} is the mole fraction of fully deprotonated EDTA, $K_{\text{f}}^{\text{Zn(II)}-\text{EDTA}}$ is the formation constant of fully deprotonated EDTA for Zn(II), a value of $10^{16.5}$, and $K_{(1-6)}$ values are the stepwise proton dissociation constants of EDTA; $K_1 = 1.0$, $K_2 = 3.1 \times 10^{-2}$, $K_3 = 1.0 \times 10^{-2}$, $K_4 = 2.2 \times 10^{-3}$, $K_5 = 6.9 \times 10^{-7}$, and $K_6 = 5.8 \times 10^{-11}$ (*38*).

Potentiometric pH Titrations. Potentiometric pH titrations of both *apo* and *holo*-**GGG** were performed using a 1.0 cm path length cuvette fitted with a pH electrode under a stream of nitrogen gas. For *holo*-**GGG**, the pH of a 25 μM Zn(II)−**GGG** sample in a combination buffer (20 mM HEPES, 20 mM MES, and 100 mM KCl) was adjusted by the addition of microliter aliquots of 0.1 N HCl. Between each addition, the samples were allowed to equilibrate for 3 min prior to measurement of the total fluorescence emission. The pH dependence of the total fluorescence was fit to an equation for two protonation events, a one proton event with an effective $\text{p}K_{\text{a1}}^{\text{eff}}$ value and a cooperative three proton protonation event with an effective $\text{p}K_{\text{a2}}^{\text{eff}}$ value.

$$Fl_{\text{meas}} = Fl_0 + \frac{\Delta Fl_1}{10^{(-\text{pK}_{\text{a1}}^{\text{eff}}+\text{pH})} + 10^{(-3\text{pH}+3\text{pK}_{\text{a2}}^{\text{eff}})} + 1} + \frac{\Delta Fl_2}{10^{(-3\text{p}K_{\text{a2}}^{\text{eff}}+3\text{pH})} + 10^{(-\text{p}K_{\text{a1}}^{\text{eff}}-3\text{p}K_{\text{a2}}^{\text{eff}}+4\text{pH})} + 1} \quad (12)$$

The total fluorescence measured at any pH, Fl_{meas}, is a function of the initial fluorescence, Fl_0, the change in fluorescence due to the first and second protonation events, ΔFl_1 and ΔFl_2, respectively, the solution pH value, and the effective acid dissociation constants of the ligands bound to metal, $\text{p}K_{\text{a1}}^{\text{eff}}$ and $\text{p}K_{\text{a2}}^{\text{eff}}$. The cooperative three proton transition effected the change in fluorescence, ΔFl_2, by ~75%, whereas the one proton transition effected the change in fluorescence, ΔFl_1, by ~25%.

For *apo*-**GGG**, the change in solution pH was monitored upon the addition of microliter aliquots of 0.5 N HCl to a 65 μM aqueous solution of **GGG** containing 100 mM KCl at pH 10.0. The titration data were best fit to a protonation model involving the ionization of seven titratable residues.

$$\frac{[\text{H}^+]}{[\textbf{GGG}]} = 7\alpha_{\text{H}_7\text{A}} + 6\alpha_{\text{H}_6\text{A}} + 5\alpha_{\text{H}_5\text{A}} + 4\alpha_{\text{H}_4\text{A}} + 3\alpha_{\text{H}_3\text{A}} + 2\alpha_{\text{H}_2\text{A}} + \alpha_{\text{HA}} + 0\alpha_{\text{A}} \quad (13)$$

$$\alpha_{\text{H}_7\text{A}} = \frac{10^{-7*\text{pH}}}{\Sigma};\ \alpha_{\text{H}_6\text{A}} = \frac{10^{-6*\text{pH}-\text{p}K_{\text{a1}}}}{\Sigma}$$

$$\alpha_{\text{H}_5\text{A}} = \frac{10^{-5*\text{pH}-\text{p}K_{\text{a1}}-\text{p}K_{\text{a2}}}}{\Sigma};\ \alpha_{\text{H}_4\text{A}} = \frac{10^{-4*\text{pH}-\text{p}K_{\text{a1}}-\text{p}K_{\text{a2}}-\text{p}K_{\text{a3}}}}{\Sigma}$$

$$\alpha_{\text{H}_3\text{A}} = \frac{10^{-3*\text{pH}-\text{p}K_{\text{a1}}-\text{p}K_{\text{a2}}-\text{p}K_{\text{a3}}-\text{p}K_{\text{a4}}}}{\Sigma};\ \alpha_{\text{H}_2\text{A}} = \frac{10^{-2*\text{pH}-\text{p}K_{\text{a1}}-\text{p}K_{\text{a2}}-\text{p}K_{\text{a3}}-\text{p}K_{\text{a4}}-\text{p}K_{\text{a5}}}}{\Sigma}$$

$$\alpha_{\text{HA}} = \frac{10^{-\text{pH}-\text{p}K_{\text{a1}}-\text{p}K_{\text{a2}}-\text{p}K_{\text{a3}}-\text{p}K_{\text{a4}}-\text{p}K_{\text{a5}}-\text{p}K_{\text{a6}}}}{\Sigma};\ \alpha_{\text{A}} = \frac{10^{-\text{p}K_{\text{a1}}-\text{p}K_{\text{a2}}-\text{p}K_{\text{a3}}-\text{p}K_{\text{a4}}-\text{p}K_{\text{a5}}-\text{p}K_{\text{a6}}-\text{p}K_{\text{a7}}}}{\Sigma} \quad (14)$$

$$\Sigma = 10^{-7*\text{pH}} + 10^{-6*\text{pH}-\text{p}K_{\text{a1}}} + 10^{-5*\text{pH}-\text{p}K_{\text{a1}}-\text{p}K_{\text{a2}}} + 10^{-4*\text{pH}-\text{p}K_{\text{a1}}-\text{p}K_{\text{a2}}-\text{p}K_{\text{a3}}} + \ldots + 10^{-\text{p}K_{\text{a1}}-\text{p}K_{\text{a2}}-\text{p}K_{\text{a3}}-\text{p}K_{\text{a4}}-\text{p}K_{\text{a5}}-\text{p}K_{\text{a6}}-\text{p}K_{\text{a7}}} \quad (15)$$

$[\text{H}^+]/[\text{GGG}]$ is the equivalents of acid added relative to the peptide. α_{HxA} is the mole fraction of a particular protonation state of *apo*-**GGG**, where $x = 0-7$, and the coefficients, 0 through 7, are the equivalents of acid required to generate 100% of a given protonation state of the peptide. $\text{p}K_{\text{ai}}$, where $i = 1-7$, is the $\text{p}K_{\text{a}}$ of a particular residue, and pH is the measured solution pH.

pH Dependence of Conditional Dissociation Constants. Because of the expected $[\text{H}^+]^4$ dependence of the Zn(II)−

GGG conditional dissociation constant, K_d values were measured at varying pH values in order to determine the value of K_f^{ML}. The K_d value at each pH was determined as described above using fluorescence spectroscopy. The resulting plot of $-\log K_d$ versus pH is fit to the following equilibrium binding expression:

$$-\log K_d = -\log\left(\frac{1}{K_f^{ML}} * \frac{1 + 10^{(-pH+pK_{a1}^{eff})} + 10^{(-4pH+pK_{a1}^{eff}+3pK_{a2}^{eff})}}{1 + 10^{(-pH+pK_{a2})} + 10^{(-2pH+pK_{a2}+pK_{a3})} + 10^{(-3pH+pK_{a2}+pK_{a3}+pK_{a4})} + 10^{(-4pH+pK_{a2}+pK_{a3}+pK_{a4}+pK_{a5})}}\right) \quad (16)$$

where the conditional dissociation constant at any pH, K_d, is a function of the pH independent association constant at high pH K_f^{ML}, where the fully deprotonated **GGG** ligand and $\{Zn(II)(H_2O)_6\}^{2+}$ associate to form the Zn(II)−**GGG** complex, the effective acid dissociation constants of the metal-bound cysteines, pK_{a1}^{eff} and pK_{a2}^{eff}, the acid dissociation constants of the cysteines in the *apo*-peptide, pK_{a2} − pK_{a5}, and the solution pH.

Isothermal Titration Calorimetry (ITC). ITC experiments were performed on an OMEGA Titration Calorimeter (Micro Cal, Inc., Northampton, MA) (*39*−*42*). Typical experiments involved the titration of microliter aliquots of a 5.0 mM stock solution of $Zn(II)Cl_2$ in unbuffered, pH 7.0 water into buffered solutions of 50−100 μM **GGG**. Under these conditions, the $Zn(II)Cl_2$ stock is predominantly $\{Zn(II)(H_2O)_6\}^{2+}$ and hydrolysis does not occur to a significant extent (*43*, *44*). In order to facilitate the direct comparison of the ITC results with those obtained from the fluorimetric titrations, the identical $Zn(II)Cl_2$ stock solution was utilized for all experiments regardless of the buffered peptide solution pH value. Because the use of a Zn(II) stock solution whose identity is not matched to the buffered peptide solution in the ITC cell may produce spurious and unaccounted heats (*42*), the heat of addition of the stock Zn(II) solution to the peptide solution after saturation of the peptide ligand was determined in each ITC experiment and subtracted from ITC data; these heats were comparable to the heats of addition of the Zn(II) stock solution to the different buffers at varying pH values in the absence of the peptide. Finally, two control ITC experiments in which the Zn(II) and peptide solutions were matched at pH 8.0 and 7.0 showed identical reaction enthalpies, within a 0.5 kcal mol^{-1} experimental error, to those measured using the unbuffered Zn(II) stock. All peptide manipulations were done anerobically, and all solvents were thoroughly degassed to prevent cysteine oxidation. The sample was maintained at 25 °C by using a ThermoNeslab refrigerated recirculating water bath as a heat sink. Titrations were conducted in triplicate using three different buffers at each of three pH values, 5.5, 7.0, and 8.0. At all pH values, 20 mM HEPES, 100 mM KCl ($\Delta H_{protonation} = -5.02$ kcal/mol), 20 mM PIPES, and 100 mM KCl ($\Delta H_{protonation} = -2.73$ kcal/mol) were used (*45*). At pH 8.0, 20 mM MOPS and 100 mM KCl ($\Delta H_{protonation} = -5.22$ kcal/mol) were also used, whereas at pH 5.5 and 7.0, 20 mM MES and 100 mM KCl ($\Delta H_{protonation} = -3.71$ kcal/mol) were used (*45*). At pH 5.5 (20 mM HEPES and 100 mM KCl), titrations were completed at 25, 35, and 65 °C for van't Hoff analysis and determination of ΔC_P. Between each experiment, the sample cell was thoroughly rinsed with 0.1 M EDTA, followed by deionized water, to ensure the complete removal of residual metal salts, EDTA, and peptide. The solution pH was checked before and after each experiment to ensure that there were no changes in pH.

Scheme 1

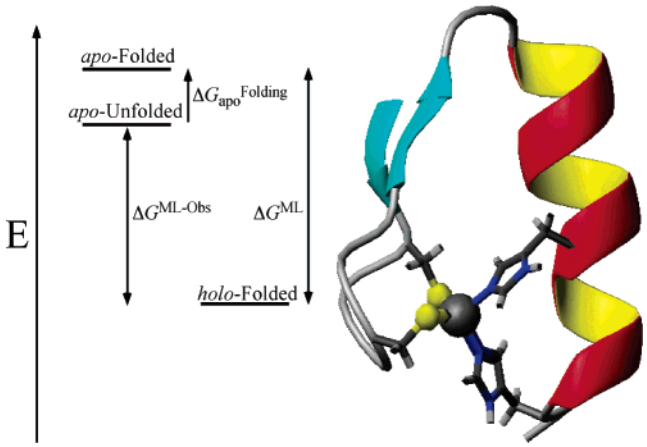

All data were analyzed using the Origin software supplied with the Micro Cal instrument (*39*). All data showed the expected 1:1 metal/peptide stoichiometry, consistent with the lack of hydrolysis and precipitation of the $\{Zn(II)(H_2O)_6\}^{2+}$ stock solution. Prior to fitting to a 1:1 equilibrium binding model, the heat of water addition to buffered peptide solution and heat of addition of aqueous $Zn(II)Cl_2$ to buffer, derived from control experiments, were subtracted from the experimental data. The reaction enthalpies were determined according to the following relationship:

$$\Delta H_{obs} = \Delta H_{rxn} + n\Delta H_{buffer\ protonation} \quad (17)$$

where ΔH_{obs} is the observed enthalpy, ΔH_{rxn} is the intrinsic reaction enthalpy, $\Delta H_{buffer\ protonation}$ is the enthalpy of buffer protonation, and n is number of protons released upon metal binding. The reaction enthalpy was determined by the y-intercept of a plot of ΔH_{obs} versus $\Delta H_{buffer\ protonation}$, and the number of protons released (n) was determined from the slope of the linear fit. The number of protons released at each pH studied matched expectations based on the speciation of the ligand and metal−ligand complex from eqs 12−15, which validates our use of an unbuffered Zn(II) stock solution. The reaction entropies were calculated on the basis of the calorimetric determination of the reaction enthalpies and the reaction free energies, ΔG_{rxn}, according to the following expression.

$$\Delta G_{rxn} = \Delta H_{rxn} - T\Delta S_{rxn} \quad (18)$$

The values of ΔG_{rxn} used in eq 18 were determined from ITC, where available, or from the analogous fluorimetric titration data.

RESULTS

Experimental Design. Zinc finger proteins are classic examples of biological macromolecules that exhibit metal induced protein folding events (*3*, *4*). Observed to be unstructured in the *apo*-state, zinc fingers fold into discrete 3D structures upon Zn(II) incorporation. Scheme 1 shows

Scheme 2

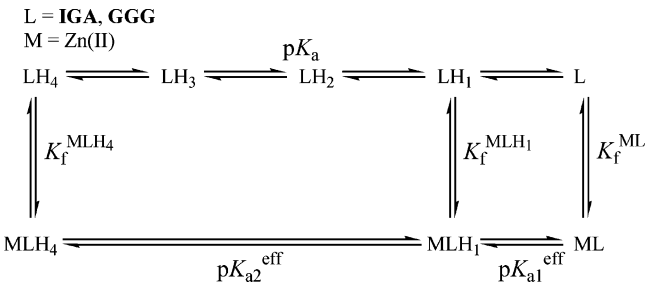

one such structure, the $\beta\beta\alpha$ fold of Zif268, and also presents a free energy diagram of a generic coupled metal-binding protein-folding event (*46*). In the absence of the metal ion, the *apo*-protein predominantly populates the ensemble of *apo*-unfolded states at lower energy than the *apo*-folded state. The energy required to fold the *apo*-protein into the correct 3D structure in the absence of metal, that is, the *apo*-folded state, is represented in Scheme 1 by $\Delta G_{apo}^{Folding}$. Upon addition of the metal ion to the *apo*-protein, the formation of the *holo*-folded state from the *apo*-unfolded state results because of the energy contributed by the metal−ligand interactions. The observed metal−ligand binding free energy, ΔG^{ML-Obs}, for the metalloprotein can be derived from the dissociation constant, K_d, using the relationship $\Delta G^{ML-Obs} = -RT \ln K_d$. However, this observed free energy is smaller than the actual metal−ligand free energy contribution, which is shown as ΔG^{ML}, that is, the energy between the *apo*-folded and *holo*-folded states. In other words, the observed metal−ligand free energy contribution, ΔG^{ML-Obs}, is equivalent to the metal−ligand contribution, ΔG^{ML}, minus the free energy required to fold the protein, $\Delta G_{apo}^{Folding}$, that is, $\Delta G^{ML-Obs} = \Delta G^{ML} - \Delta G_{apo}^{Folding}$. Because metal ion binding and protein folding are coupled, it has proven difficult to parse apart the energetic cost of protein folding or the actual contribution of metal-ion binding. In the case of a classical 26 amino acid designed zinc finger protein, $\Delta G_{apo}^{Folding}$ has been estimated to be as high as +16 kcal mol^{-1} on the basis of the structure-based thermodynamic analysis set forth by Blaise and Berg (*47*).

In order to determine values of ΔG^{ML} for structural metal-ion sites, our approach is to minimize the energy difference between the *apo*-folded and *apo*-unfolded states by using simple, unstructured, monomeric peptides so that ΔG^{ML-Obs} and ΔG^{ML} become nearly equivalent. Previously, we developed a 16 amino acid peptide containing four cysteine residues, **IGA**, on the basis of the consensus sequence of ferredoxin proteins that binds a [4Fe-4S] cluster and acts as a ferredoxin maquette (*18*). More recently, we have shown that the tetrahedral, tetrathiolate coordination site in **IGA** is an avid binder of Zn(II) and is selective for this metal over Co(II) and Fe(II) (*21*).

On the basis of previous contributions from those characterizing metal−protein interactions (*42*, *48*), we have developed a suite of equilibrium measurements using the **IGA** peptide to determine the pH independent Zn(II)−**IGA** formation constant K_f^{ML} from which ΔG^{ML} can be derived (*21*). Because the formation of Zn(II)−**IGA** involves proton release, the pH dependence of Zn(II)−**IGA** complex formation was used to determine K_f^{ML}. Scheme 2 shows the minimal set of equilibria involved in the formation of Zn(II)−**IGA** from the *apo*-peptide and $\{Zn(II)(H_2O)_6\}^{2+}$. The

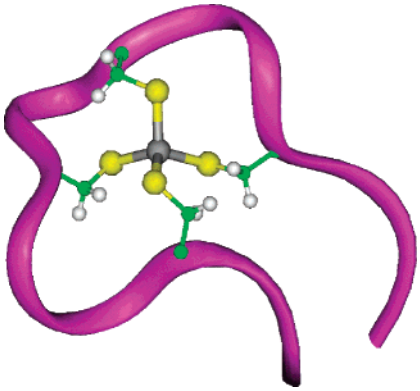

FIGURE 1: Molecular model of the Zn(II)−**GGG** complex rendered using Biosym Insight II.

effective acid dissociation constants of the ligands bound to the metal, that is, the pK_a^{eff} values, are determined using potentiometric titrations that reveal the pH stability of the metallopeptide. The pK_a values of the cysteine ligands in the absence of the metal were assumed to be 8.3, the solution pK_a value of free cysteine. The dissociation constant of the Zn(II)−**IGA** complex at various solution pH values were determined using equilibrium binding titrations. These conditional dissociation constants were fit to an expression for the underlying equilibria involving protons and metal-ion binding to the peptide ligands shown in Scheme 2, which at high pH yields the value of the pH independent formation constant, K_f^{ML}, of the Zn(II)−**IGA** complex. The fit at low pH gives the pH independent formation constant $K_f^{MLH_4}$ of the metallopeptide with protonated ligands, that is, Zn(II)−**IGA**-$4H^+$. Ultimately, this thermodynamic analysis provided the K_f^{ML} value of Zn(II)−**IGA**, determined to be 8.0×10^{15} M^{-1}, or a K_d value of 125 aM, which rivals the tightest natural Zn(II) proteins and demonstrates that ΔG^{ML} is favorable by at least −21.7 kcal mol^{-1}.

In this study, we utilize a variant of **IGA** to elucidate the thermodynamic affinity of a Cys_4 site for Zn(II) and to evaluate the impact of proton release on the entropic and enthalpic contributions of a Zn(II)−$(S{\cdot}Cys)_4$ site toward metalloprotein stability. Because the sequence of **IGA** contains an isoleucine and an alanine residue derived from the ·C**IG**CG**A**C· consensus motif of bacterial ferredoxins (*18*, *21*), we replaced these with more flexible glycine residues, which are more commonly found in Zn(II) proteins, in an effort to more closely emulate structural Zn(II) sites such as the one found in alcohol dehydrogenase as well as to discourage the formation of any secondary structural elements (*1*). Figure 1 shows a molecular model of the peptide used for this study, **GGG**, which has the primary structure NH_2-KLCEGG·C**GG**CG**G**C·GGW-$CONH_2$ and is named for the non-coordinating amino acids in bold. Using a combination of Zn(II) titrations into **GGG** with and without the competing chelator EDTA, the conditional dissociation constants of Zn(II)−**GGG** were measured by fluorescence over a wide pH range. Isothermal titration calorimetry measurements, conducted in the same manner as the fluorescence titration K_d determinations, give the enthalpies of Zn(II)−**GGG** formation and, when coupled to the ΔG_{rxn} values derived from the K_d values measured by fluorescence, yield the entropies of Zn(II) coordination to **GGG**. These data are coupled with the pK_a and pK_a^{eff} values measured using potentiometric titrations of **GGG** and Zn(II)−**GGG**,

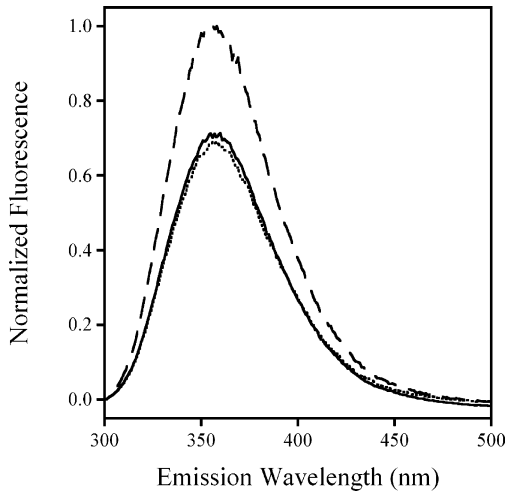

FIGURE 2: Normalized steady-state fluorescence emission spectra of 10 μM *apo*-**GGG** (····), 10 μM Zn(II)−**GGG** (---), and 10 μM Zn(II)−**GGG** with 100 μM EDTA (—) in pH 7.0 buffer (20 mM HEPES and 100 mM KCl). The peptide was excited through a 5 nm slit width at 280 nm, corresponding to the tryptophan λ_{max} value, and the fluorescence emission was collected through a 5 nm emission slit width.

respectively, to provide for the determination of the Zn(II)−**GGG** formation constant, K_f^{ML}, and the corresponding free energy of complex formation, ΔG^{ML-Obs}. A comparison of the ΔG^{ML-Obs} values between Zn(II)−**GGG** and Zn(II)−**IGA** is used to reveal whether either has significant protein folding effects upon metal-ion binding. Most importantly, differences between the ΔG^{ML-Obs} values observed for natural Zn(II)−$(S^{-}Cys)_4$ metalloproteins with metal induced protein folding events and Zn(II)−**GGG** are used to determine the cost of protein folding in the former, a set of values which have not been previously experimentally accessible.

Isothermal Titration Fluorimetry. Figure 2 shows the steady-state fluorescence emission spectrum of **GGG** and Zn(II)−**GGG** at 10 μM concentration in aqueous buffer, which demonstrates that Zn(II) binding results in an increase in tryptophan fluorescence emission. Since cysteine thiols are efficient quenchers of tryptophan fluorescence because of a collisional quenching mechanism, the deprotonation of the thiols as well as the imposition of a constraint on the sulfur atoms upon Zn(II) binding results in the observed 30% enhancement of the fluorescence emission of a C-terminal tryptophan in **GGG** (*49*). In addition, the position of the emission maximum, 357 nm, indicates that the tryptophan is solvent exposed and does not shift with Zn(II) incorporation, consistent with the design of Zn(II)−**GGG** (*50*). Figure 2 also shows the fluorescence emission spectrum of Zn(II)−**GGG** upon the addition of 10 equiv of EDTA, a Zn(II) chelator. The loss of the fluorescence enhancement due to Zn(II) binding to **GGG** is apparent and fully consistent with the removal of the Zn(II) from **GGG** by EDTA under these conditions.

Because the coordination of Zn(II) to the tetracysteine peptide **GGG** potentially releases four protons, the conditional dissociation constants for Zn(II)−**GGG** were measured over the pH range of 4.5 to 9.0. Figure 3 shows a representative equilibrium binding isotherm for the fluorescence titration of $Zn(II)Cl_2$ in unbuffered aqueous solution at pH 7.0 into 30 μM **GGG** buffered at pH 5.5 (20 mM HEPES and 100 mM KCl). The fit to the data indicates a

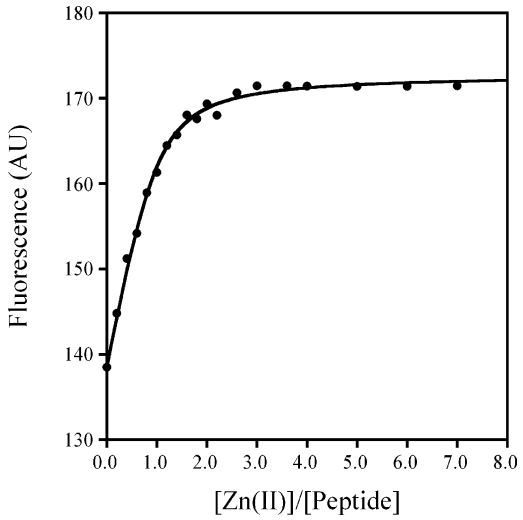

FIGURE 3: Equilibrium binding isotherm for the fluorescence detected titration of $Zn(II)Cl_2$ in unbuffered aqueous solution at pH 7.0 into 30 μM **GGG** buffered at pH 5.5 (20 mM HEPES and 100 mM KCl). A fit to the plot of the fluorescence emission intensity at 357 nm vs equivalents of Zn(II) to the peptide indicates a Zn(II)−**GGG** conditional dissociation constant, K_d, value of 4.0 μM at pH 5.5.

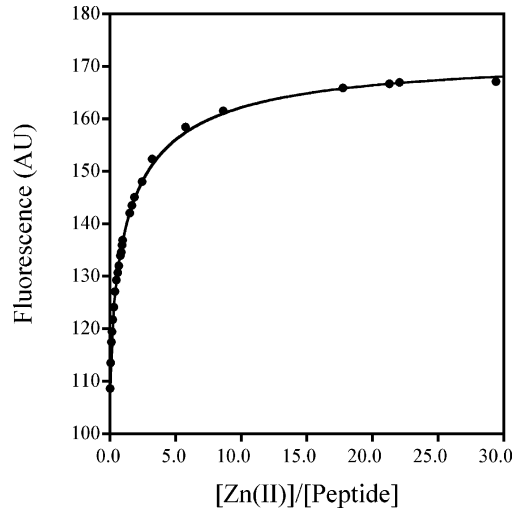

FIGURE 4: Equilibrium binding isotherm for the fluorescence detected competition titration of $Zn(II)Cl_2$ in unbuffered aqueous solution at pH 7.0 into a buffered aqueous solution at pH 8.0 (20 mM HEPES and 100 mM KCl) containing 25 μM **GGG** and 20 μM EDTA. Under these conditions, a fit to the plot of fluorescence at 357 nm vs equivalents of Zn(II) added to the peptide using eq 6 gives a competition constant value of 2.5 between **GGG** and EDTA. Because the K_d of Zn(II)-EDTA at this pH value is 2.5 fM, the resulting Zn(II)−**GGG** dissociation constant at pH 8.0 is 1.0 fM.

conditional dissociation constant, K_d, value of 4.0 μM at pH 5.5. Conditional dissociation constant measurements for Zn(II)−**GGG** were accomplished by direct $Zn(II)Cl_2$ titration into the peptide between pH 5.0 and 6.0. At pH values above 6.0, accurate K_d determinations necessitated the use of the competing chelator EDTA, whose affinity at each pH value was calculated using eqs 9−11. Figure 4 shows the competition titration of $Zn(II)Cl_2$ in unbuffered aqueous solution at pH 7.0 into a buffered aqueous solution (20 mM HEPES, 100 mM KCl) containing 25 μM **GGG** and 20 μM EDTA at pH 8.0. Under these conditions, the competition constant between **GGG** and EDTA was determined to be 2.5. Because the K_d of Zn(II)-EDTA at this pH value is 2.5 fM, the data

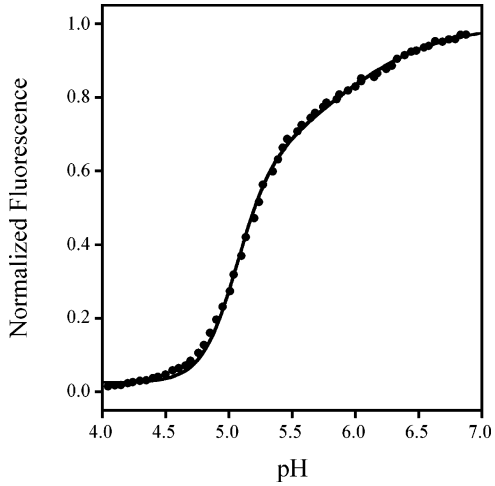

FIGURE 5: Fluorescence detected potentiometric pH titration of 30 μM Zn(II)−**GGG**. The decrease in total tryptophan fluorescence as the pH is lowered by the addition of microliter aliquots of 0.1 N HCl is due to protonation of the Zn(II)-bound thiolate ligands to form thiols. The pH titration data is best fit to an equilibrium model involving two protonation events, a one proton event at a pK_{a1}^{eff} value of 5.8 and a cooperative three proton event at a pK_{a2}^{eff} value of 5.1.

indicate that Zn(II)−**GGG** has a 1.0 fM dissociation constant at pH 8.0, a value that is on par with the extreme thermodynamics of the femtomolar Zn(II) binder, ZntR (*51*, *52*). This 1.0 fM K_d is the tightest dissociation constant measured for a peptide-based tetrathiolate Zn(II) binding site at pH 8.0.

Potentiometric pH Titrations. In order to evaluate the pH dependent chemical speciation of *apo*- and *holo*-**GGG**, potentiometric pH titrations were performed. Figure 5 shows that upon titration of 0.1 N HCl into 30 μM Zn(II)−**GGG**, there is a decrease in tryptophan fluorescence because of the protonation of the Zn(II)-bound thiolate ligands to form thiols. The pH titration of Zn(II)−**GGG** is best fit to an equilibrium model involving two protonation events, a one proton event at a pK_{a1}^{eff} value of 5.8 and a cooperative three proton event at a pK_{a2}^{eff} value of 5.1. The pK_a^{eff} values measured for the Zn(II)−**GGG** complex are similar to the Zn(II)-bound cysteine pK_a^{eff} values of Zn(II)−**IGA**, HIV-1 nucleocapsid protein, and the putative zinc finger sequence of primase (*21*, *53*−*55*). These results indicate that at pH 7.0, all four Zn(II)-bound cysteines are deprotonated thiolates, contrary to *ab initio* quantum chemical studies that suggest that structural Zn(II)−Cys_4 sites have at least one protonated Zn(II)-bound cysteine at neutral pH (*56*).

$$pK_{a2}^{eff}\ \text{Zn(II)}-\mathbf{GGG}\text{-}4H^+ \rightleftharpoons \text{Zn(II)}-\mathbf{GGG}\text{-}H^+ + 3\ H^+ \quad (19)$$

$$pK_{a1}^{eff}\ \text{Zn(II)}-\mathbf{GGG}\text{-}H^+ \rightleftharpoons \text{Zn(II)}-\mathbf{GGG} + H^+ \quad (20)$$

Figure 6 shows the pH dependent chemical speciation of the Zn(II)−**GGG** complex as revealed by the pH titration data. At pH values greater than 5.8, the major species in solution is the tetrathiolate−Zn(II) complex (solid line), Zn(II)−**GGG**; at pH values between 5.8 and 5.1, the major species in solution is the monothiol−trithiolate−Zn(II) complex (dotted line), Zn(II)−**GGG**-H^+; and at pH values below 5.1, the predominant species in solution is the tetrathiol−Zn(II) complex (dashed line), Zn(II)−**GGG**-$4H^+$, which dissociates

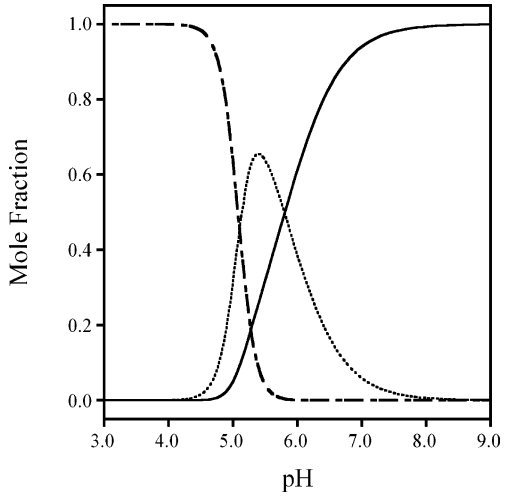

FIGURE 6: Speciation diagram of the Zn(II)−**GGG** metal−ligand complex depicting the tetrathiolate zinc species (—), Zn(II)−**GGG**, the monothiol-trithiolate zinc species (····), Zn(II)−**GGG**-H^+, and the tetrathiol zinc species (---), Zn(II)−**GGG**-$4H^+$. The diagram was generated on the basis of the protonation behavior of the Zn(II)−**GGG** complex in Figure 5.

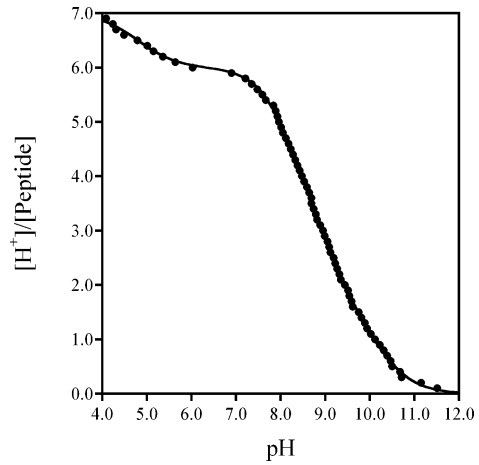

FIGURE 7: Potentiometric pH titration of **GGG**. The solution pH was monitored as microliter aliquots of 0.5 N HCl were added to an aqueous solution of 65 μM **GGG**, containing 100 mM KCl at pH 10.0. The pH titration data is best fit to an equilibrium model involving seven protonation events: $pK_{a1} = 4.8$, $pK_{a2} = 7.8$, $pK_{a3} = 8.1$, $pK_{a4} = 8.7$, $pK_{a5} = 9.0$, $pK_{a6} = 9.6$, and $pK_{a7} = 10.5$. pK_{a1} is ascribed to the glutamic acid residue, whereas pK_{a2}−pK_{a5} are ascribed to the cysteine ligands of the peptide, and pK_{a6} and pK_{a7} are the N-terminus and the epsilon amine of lysine, respectively.

into $\{Zn(II)(H_2O)_6\}^{2+}$ and **GGG**-$4H^+$ under the conditions of the experiment (*vide infra*). Thus, the potentiometric pH titration of Zn(II)−**GGG** defines the three metal−ligand species that are present over the pH range studied.

Figure 7 shows that upon titration of 0.5 N HCl into 65 μM **GGG**, the change in solution pH is best fit to an equilibrium model involving seven protonation events; $pK_{a1} = 4.8$, $pK_{a2} = 7.8$, $pK_{a3} = 8.1$, $pK_{a4} = 8.7$, $pK_{a5} = 9.0$, $pK_{a6} = 9.6$, and $pK_{a7} = 10.5$. pK_{a1} are ascribed to the glutamic acid residue, whereas pK_{a2}−pK_{a5} are ascribed to the cysteine ligands of the peptide, and pK_{a6} and pK_{a7} are the N-terminus and the epsilon amine of lysine, respectively. It is these cysteine pK_a values that are responsible for the $[H^+]^4$ dependence on the condition dissociation constant of Zn(II)−**GGG**; therefore, it is just these pK_a values that are used in the equilibrium expression that models the pH

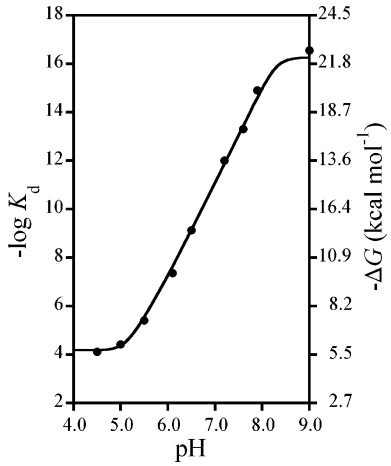

FIGURE 8: pH dependence of the conditional dissociation constant of Zn(II) complexation by **GGG**, shown as a plot of the negative logarithm of the dissociation constant or the reaction free energy vs solution pH. The equilibrium binding model employed to fit the data yields a pH independent formation constant, K_f^{ML}, value of 1.7×10^{16} M^{-1}, or a limiting dissociation constant of 60 aM, which corresponds to a reaction free energy of -22.1 kcal mol^{-1}.

dependence of the Zn(II)−**GGG** conditional dissociation constants (*vide infra*).

pH Dependence of the Conditional Dissociation Constants. Solution pH dictates not only the speciation of the Zn(II)−**GGG** complex as shown in Figure 6 but also the speciation of the **GGG** *apo*-peptide ligand and the metal, $\{Zn(II)(H_2O)_6\}^{2+}$. In terms of the Zn(II)−**GGG** complex, three species are observed, Zn(II)−**GGG**-xH$^+$, where $x = 0$, 1, or 4. In terms of the metal, aqueous Zn(II) exists as $\{Zn(II)(H_2O)_6\}^{2+}$ at pH values below 9.0 (*38*). The minimal set of equilibria required to describe the reaction of $\{Zn(II)(H_2O)_6\}^{2+}$ with **GGG**-xH$^+$ to form Zn(II)−**GGG**-xH$^+$, where $x = 0$, 1, or 4, reduces to those shown in Scheme 2 for all pH values studied. Thus, the conditional K_d value measured at a particular pH is a function of these equilibria and the reactions given below.

$$\mathbf{pH} > pK_a > pK_{a1}^{eff} > pK_{a2}^{eff}$$
$$Zn(II) + \mathbf{GGG} \rightleftharpoons Zn(II)-\mathbf{GGG} \quad (21)$$

$$pK_a > \mathbf{pH} > pK_{a1}^{eff} > pK_{a2}^{eff}$$
$$Zn(II) + \mathbf{GGG}\text{-}4H^+ \rightleftharpoons Zn(II)-\mathbf{GGG} + 4H^+ \quad (22)$$

$$pK_a > pK_{a1}^{eff} > \mathbf{pH} > pK_{a2}^{eff}$$
$$Zn(II) + \mathbf{GGG}\text{-}4H^+ \rightleftharpoons Zn(II)-\mathbf{GGG}\text{-}H^+ + 3H^+ \quad (23)$$

$$pK_a > pK_{a1}^{eff} > pK_{a2}^{eff} > \mathbf{pH}$$
$$Zn(II) + \mathbf{GGG}\text{-}4H^+ \rightleftharpoons Zn(II)-\mathbf{GGG}\text{-}4H^+ \quad (24)$$

Figure 8 shows a plot of the pH dependence of the negative logarithm of all of the conditional dissociation constant values, K_d, measured for Zn(II)−**GGG**. Using the equilibria in Scheme 2, the equilibrium binding expression in eq 16 was derived to fit the conditional K_d versus pH data. At high pH, the fit levels out at the value of the pH independent formation constant, K_f^{ML}, for Zn(II)−**GGG**, which corresponds to the formation of the Zn(II)−**GGG** complex from the deprotonated ligand, **GGG**, and $\{Zn(II)(H_2O)_6\}^{2+}$. The fit to the data, which takes into account the potentiometrically determined cysteine pK_a values of *apo* and *holo*-**GGG**, pK_a and pK_a^{eff}, respectively, gives a K_d^{ML} value of 60 aM, or a K_f^{ML} value of 1.7×10^{16} M^{-1}, which indicates that Zn(II) binding to **GGG** contributes 22.1 kcal/mol to metalloprotein stability because $\Delta G^{ML-Obs} = -RT \ln K_f^{ML}$. Furthermore, this 60 aM dissociation constant is on par with the tightest natural Zn(II) binding proteins (*51*, *52*, *57*). The K_d value determined at pH 9.0 for the Zn(II)−**GGG** complex is 30 aM, and is within the experimental error of the 60 aM number derived from the fit to the K_d−pH plot.

As the pH is lowered below the pK_a values of the cysteines in the free ligand, corresponding to pK_{a2}−pK_{a5} in the potentiometric pH titration of *apo*-**GGG**, the conditional dissociation constants become attenuated by proton competition, exhibiting a $[H^+]^4$ dependence because the reaction progresses to one where **GGG**-4H$^+$ binds $\{Zn(II)(H_2O)_6\}^{2+}$ to form Zn(II)−**GGG** with the release of four protons (*58*). As the solution pH approaches the effective pK_a values of the Zn(II)-bound thiolates, pK_{a1}^{eff} and pK_{a2}^{eff}, the products of the reaction are the protonated complexes, Zn(II)−**GGG**-H$^+$ and Zn(II)−**GGG**-4H$^+$. Under these conditions, the conditional K_d values have a pH dependency that is weaker than $[H^+]^4$. As the solution pH is lowered below pK_{a2}^{eff}, the reaction becomes pH-independent because both the reactant, **GGG**-4H$^+$, and the product, Zn(II)−**GGG**-4H$^+$, are protonated, and the fit levels out to the value of the formation constant of the Zn(II)−**GGG**-4H$^+$ complex, K_f^{MLH4}. The fit to the data yields a pH independent K_d^{MLH4} value of 75 μM or a K_f^{MLH4} value of 1.4×10^4 M^{-1}, which indicates that although thiols have significant affinity for Zn(II), the metal dissociates from the Zn(II)−**GGG**-4H$^+$ complex under our typical reaction conditions of 25 μM peptide.

Isothermal Titration Calorimetry. In order to determine the impact of protons on the enthalpic and entropic contributions to the free energies of binding, we employed isothermal titration calorimetry (ITC) at three pH values, 5.5, 7.0, and 8.0. These pH values were chosen because of the differences in the number of protons released upon Zn(II) complexation by the peptide; on the basis of the expectations from the speciation of the free ligand and metal−ligand complex, 3.2, 3.8, and 2.5 protons are predicted to be released at pH values of 5.5, 7.0, and 8.0, respectively.

Under ideal conditions, ITC has the potential to directly measure both the free energy and enthalpy of a reaction, and thus the reaction entropy (*39*−*42*). Figure 9 shows the thermogram and equilibrium binding isotherm of $ZnCl_2$ titrated into 50 μM **GGG** at pH 5.5. The binding isotherm shows the expected 1:1 stoichiometry, and a fit of the data to a 1:1 binding model yields a conditional K_d value of 4.0 μM ($\Delta G_{rxn} = -7.4$ kcal mol^{-1}). This conditional K_d value is identical to that determined by fluorimetry under the same conditions, demonstrating that both experimental techniques are comparable as well as validating the use of unbuffered $ZnCl_2$ in the ITC experiments to match the conditions used in the fluorimetric titration.

The observed enthalpy of Zn(II) complexation by the peptide, ΔH_{obs}, is the sum of the reaction enthalpy, ΔH_{rxn}, and the buffer protonation enthalpy, $\Delta H_{buffer\ protonation}$, weighted by the number of protons involved in protonating the buffer, n. The value of ΔH_{rxn} at each pH studied was determined by measuring ΔH_{obs} in three different buffer systems with

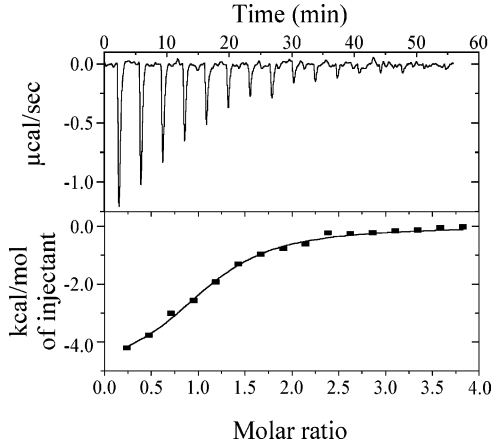

FIGURE 9: ITC derived equilibrium binding thermogram of $ZnCl_2$ in unbuffered aqueous solution at pH 7.0 titrated into 50 μM **GGG** at pH 5.5 (20 mM MES and 100 mM KCl). The thermogram shows the expected 1:1 stoichiometry of Zn(II) complexation. A fit of the data to a 1:1 binding model yields a conditional K_d value of 4.0 μM or a ΔG_{rxn} value of -7.4 kcal mol^{-1}.

Table 1: Thermodynamics of Zn(II)−**GGG** Formation at 298 K

	pH 5.5	pH 7.0	pH 8.0
$\Delta G°$ kcal mol^{-1}	−7.4	−15.1	−20.2
$\Delta H°$ kcal mol^{-1}	7.7	6.4	−2.0
$-T\Delta S°$ kcal mol^{-1}	−15.1	−21.5	−18.2
H^+ released	3.2	3.8	2.5

varying protonation enthalpies. The application of a linear regression analysis to a plot of ΔH_{obs} versus $\Delta H_{buffer\ protonation}$ gives both ΔH_{rxn} and n as the y-intercept and slope, respectively. At pH 5.5, ΔH_{rxn} was determined to be +7.7kcal mol^{-1}, and n was found to be 2.9, matching, within experimental error, the expectations based on the speciation of the ligand and metal−ligand complex deduced from the fluorescence and potentiometric titration data. According to the relationship between the free energy, enthalpy, and temperature of the reaction given in eq 18, the reaction entropy of Zn(II) complexation was calculated on the basis of the ITC determined free energy and enthalpy of reaction at 25 °C and determined to be +51.0 cal K^{-1} mol^{-1}. Thus, at pH 5.5, Zn(II) complexation by the peptide is favorable by −7.4 kcal mol^{-1} (ΔG_{rxn}), endothermic by +7.7 kcal mol^{-1} (ΔH_{rxn}), and entropically driven by −15.1 kcal mol^{-1} at 25 °C ($-T\Delta S_{rxn}$) (Table 1).

Because ITC experiments at pH 5.5 are able to accurately measure the Zn(II)−**GGG** dissociation constant and reaction enthalpies, experiments were performed at three different temperatures, 25, 35, and 65 °C, to determine the reaction entropies and enthalpies from a van't Hoff analysis. A linear regression analysis of a plot of ln K_d^{-1} versus T^{-1} yields a ΔH_{rxn} value of +8.0 kcal mol^{-1} and a ΔS_{rxn} value of +51.7 cal K^{-1} mol^{-1} as the slope and y-intercept, respectively. These values are similar to the enthalpy and entropy determined by ITC at 25 °C, ΔH_{rxn} of +7.7 kcal mol^{-1} and ΔS_{rxn} of +51.0 cal K^{-1} mol^{-1}, indicating that the ΔC_p of the Zn(II) complexation reaction is negligible. The temperature dependence of the reaction enthalpy yields a ΔC_p value of −15 cal K^{-1} mol^{-1}, which is consistent with the absence of significant structural changes in the protein scaffold upon Zn(II) coordination, as expected for a simple, unstructured peptide. A similar negligible ΔC_p value of 10 cal K^{-1} mol^{-1} is observed for a natural Cys_3His zinc finger, the HIV-1 nucleocapsid protein, which is relatively unstructured in both its *apo*- and *holo*-states, whereas the designed Cys_2His_2 zinc finger, CP-1, which adopts a $\beta\beta\alpha$ fold upon Zn(II) coordination, has a ΔC_p value of −514 cal K^{-1} mol^{-1} (*47*, *59*). Thus, the ΔC_p value of Zn(II)−**GGG** likely reflects its lack of significant secondary structure in both the *apo*- and *holo*-states.

At higher pH values, the ITC derived thermograms only allowed for the determination of ΔH_{rxn} because the complexation of Zn(II) by the peptide was too tight to accurately determine conditional K_d values. In these cases, the fluorimetrically derived dissociation constants were used to determine the ΔG_{rxn} values. At pH 7.0, the calorimetrically determined reaction enthalpy, ΔH_{rxn}, of +6.4 kcal mol^{-1} was combined with the ΔG_{rxn} value of −15.1 kcal mol^{-1}, corresponding to a conditional K_d value of 8.0 pM, to yield a reaction entropy of +72 cal K^{-1} mol^{-1} or −21.5 kcal mol^{-1} at 25 °C ($-T\Delta S_{rxn}$) (Table 1). The entropy driven complexation of Zn(II) by a thiolate rich peptide at pH 7.0 is not unique to **GGG** because it is also observed in the Cys_3His HIV-1 nucleocapsid protein, whose thermodynamic parameters are coincidentally identical, within error, to Zn(II)−**GGG** (*59*). The buffer dependent observed reaction enthalpy also revealed the release of 3.9 protons upon Zn(II) complexation, again matching expectations based on the chemical speciation of the ligand and metal−ligand complex, within error. The +21.0 cal K^{-1} mol^{-1} increase in reaction entropy or −6.4 kcal mol^{-1} at 25 °C ($-T\Delta S_{rxn}$) between the pH values of 5.5 and 7.0 reflects the impact of metal induced proton release on the reaction entropy because the difference in proton release between the two pH values is one proton. At pH 7.0, the reaction of $\{Zn(II)(H_2O)_6\}^{2+}$ with **GGG**-4H$^+$ releases 4.0 protons to form Zn(II)−**GGG.** At pH 5.5, the same reaction releases a total of 3.2 protons as it forms Zn(II)−**GGG**-4H$^+$ (4% of zero proton release), Zn(II)−**GGG**-H$^+$ (64% of three proton release), and Zn(II)−**GGG** (32% of four proton release).

At pH 8.0, where the **GGG**-4H$^+$ reactant is partially deprotonated prior to Zn(II) binding, the ITC data gives a slightly exothermic reaction enthalpy of −2.0 kcal mol^{-1}. The ΔH_{rxn} value of −2.0 kcal mol^{-1} can be combined with the fluorimetrically derived ΔG_{rxn} value of −20.2 kcal mol^{-1}, corresponding to a K_d value of 1.0 fM, to give a reaction entropy of +61 cal K^{-1} mol^{-1} or −18.2 kcal mol^{-1} at 25 °C ($-T\Delta S_{rxn}$). The data also reveals the release of 2.0 protons upon Zn(II) complexation, which matches expectations based on the speciation of the ligand and metal−ligand complex, within a 0.5 proton error (Table 1). The entropic contribution to Zn(II) complexation at pH 8.0, +61.0 cal K^{-1} mol^{-1}, is attenuated by +11 cal K^{-1} mol^{-1} relative to complexation at pH 7.0, reflecting the decrease in proton release upon metal binding.

In toto, the ITC data evince that in the pH region between 5.5 and 8.0, that is, between the pK_a^{eff} and pK_a values, Zn(II) complexation by **GGG** is entropically driven, with all of the thermodynamic values modulated by proton release. At pH 5.5, where 3.2 protons are released, the reaction entropy is +51.0 cal K^{-1} mol^{-1}; at pH 7.0, where 3.8 protons are released, the reaction entropy plateaus at a maximum value of +72.0 cal K^{-1} mol^{-1}; and at pH 8.0, where 2.5 protons are released, the entropy attenuates to +61.0 cal K^{-1}

mol^{-1} (Table 1). In addition to the proton release from cysteine, water release from both the peptide scaffold and the metal likely play a significant role in modulating the observed enthalpy and entropy values.

DISCUSSION

The influence of protons on the thermodynamic contribution of a Zn(II)−(S·Cys)$_4$ site toward metalloprotein stability has been evaluated using the pH dependence of Zn(II) binding to a simple, unstructured, model peptide containing four metal-coordinating cysteine residues, **GGG**. Using a suite of equilibrium measurements, the solution speciation of the Zn(II)−**GGG** complex is elucidated over the pH range of 4.5 to 9.0. The data indicate that Zn(II)−**GGG** formation is entropy driven and possesses a limiting K_d^{ML} value of 60 aM. The corresponding −22.1 kcal mol^{-1} limiting free energy of Zn(II) binding to **GGG** is both an order of magnitude larger than typical protein−protein interactions and significantly larger than the folding free energy of many natural proteins (*60*). This formation constant is attenuated at pH values below the pK_a of the cysteines in the *apo*-peptide because of proton competition, and the 8.0 pM conditional dissociation constant of Zn(II)−**GGG** measured at pH 7.0, is nearly identical to the values reported for natural and synthetic zinc finger proteins at the same pH. By coupling the pH dependence of the conditional K_d values with the acid dissociation constants of the *apo*-peptide, pK_a, and *holo*-peptide, pK_a^{eff}, we have mapped out the role of protons in the solution speciation and formation of Zn(II)−**GGG**. Depending on the solution pH relative to the pK_a and pK_a^{eff} values, the reaction of $\{Zn(II)(H_2O)_6\}^{2+}$ with *apo*-peptide yields one or more of the following complexes: Zn(II)−**GGG**, Zn(II)−**GGG**-H$^+$, and Zn(II)−**GGG**-4H$^+$. At solution pH values above the pK_a and pK_a^{eff} values, the reaction of $\{Zn(II)(H_2O)_6\}^{2+}$ with deprotonated **GGG** yields Zn(II)−**GGG** with a limiting K_d^{ML} value of 60 aM, which is both entropically and enthalpically favored. At pH 7.0, that is, between the values of pK_a and pK_a^{eff}, the reaction of $\{Zn(II)(H_2O)_6\}^{2+}$ with protonated **GGG**-4H$^+$ also yields Zn(II)−**GGG** but is enthalpically disfavored because of the necessity to break the four cysteine S−H bonds and more entropically favored because of the release of the four protons relative to the reaction at pH 8.0. At pH 5.5, between the pK_{a1}^{eff} and pK_{a2}^{eff} values, a combination of all three complexes are formed with the major product being Zn(II)−**GGG**-H$^+$ with a mole fraction of 0.6. Because there are multiple products, the changes in entropy and enthalpy cannot be isolated to a single species. However, it is evident that the reaction is more enthalpically and entropically disfavored at pH 5.5 relative to that at pH 7.0. Although this is consistent with the loss of only three protons at pH 5.5, it also includes energetic terms because of diminished water release from the peptide scaffold upon Zn(II) complexation, possible incomplete Zn(II) dehydration upon peptide coordination, and the weaker interaction between the Zn(II) and the protonated thiols.

While it would appear that the favorability of the reaction entropy tracks with the number of protons released, implying that proton release is entropically favorable, the calorimetric determination of the enthalpy and entropy of free cysteine thiol deprotonation are both thermodynamically unfavorable, exhibiting a positive enthalpy, $\Delta H_{\text{cys deprotonation}} = +8.6$ kcal mol^{-1} and negative entropy, $\Delta S_{\text{cys deprotonation}} = -9.0$ cal K^{-1} mol^{-1} (*61*). If the enthalpy and entropy of cysteine deprotonation in a peptide based chelator are the same as those in free cysteine, as assumed by Blaise and Berg in their structure-based thermodynamic analysis of metal-induced protein folding (*47*), then proton release upon metal binding does not contribute favorably to the reaction entropy. Thus, their analysis indicates that the observed modulation in entropy as a function of pH is not directly due to proton release. An alternative interpretation of the data is that peptide dehydration tracks with the protonation state of the *apo*-peptide, that is, at pH 8.0, where the cysteines are partially deprotonated, desolvation is more entropically unfavorable than at pH 7.0, where the cysteines are protonated. If Zn(II) dehydration and the structure of Zn(II)−**GGG** are constant between pH 7.0 and 8.0, the difference in the measured enthalpy and entropy values reflects the differences in cysteine proton release, Δn, and water release from the *apo*-peptide scaffold upon Zn(II) complexation (eqs 25 and 26).

$$\Delta\Delta H_{\text{rxn}} = \Delta H_{\text{rxn}}^{7.0} - \Delta H_{\text{rxn}}^{8.0} = \Delta n \Delta H_{\text{cys deprotonation}} + \Delta\Delta H_{\text{peptide dehydration}} \quad (25)$$

$$\Delta\Delta S_{\text{rxn}} = \Delta S_{\text{rxn}}^{7.0} - \Delta S_{\text{rxn}}^{8.0} = \Delta n \Delta S_{\text{cys deprotonation}} + \Delta\Delta S_{\text{peptide dehydration}} \quad (26)$$

$\Delta H_{\text{rxn}}^{\text{pH}}$ and $\Delta S_{\text{rxn}}^{\text{pH}}$ are the enthalpy and entropy of the reaction, respectively, measured at a pH value (7.0 or 8.0), Δn is the difference in the number of protons released between these pH values, $\Delta\Delta H_{\text{peptide dehydration}}$ and $\Delta\Delta S_{\text{peptide dehydration}}$ are the difference in the enthalpy and entropy of peptide dehydration between these pH values, and $\Delta H_{\text{cys deprotonation}}$ and $\Delta S_{\text{cys deprotonation}}$ are the enthalpy and entropy of proton dissociation from the cysteine thiol. With an enthalpy difference between pH 7.0 and 8.0 of +8.4 kcal mol^{-1} ($\Delta H_{\text{rxn}}^{7.0} - \Delta H_{\text{rxn}}^{8.0}$), Δn equal to 1.8, and the $\Delta H_{\text{cys deprotonation}}$ equal to +8.6 kcal mol^{-1} (*58*), the calculated difference in the $\Delta H_{\text{peptide dehydration}}$ between pH 7.0 and 8.0 is equal to −7.1 kcal mol^{-1}. Similarly, with the entropy difference between pH 7.0 and 8.0, $\Delta\Delta S_{\text{rxn}}$, equal to 11 cal K^{-1} mol^{-1}, Δn equal to 1.8, and the $\Delta S_{\text{cys deprotonation}}$ equal to −9.0 cal K^{-1} mol^{-1} (*58*), the difference in $\Delta S_{\text{peptide dehydration}}$ can be calculated to be 27 cal K^{-1} mol^{-1}. Thus, at 298 K, it is energetically more favorable by −15.1 kcal mol^{-1}, that is, −7.1 kcal mol^{-1} − (298 K × 0.027 kcal K^{-1} mol^{-1}), to dehydrate the peptide upon Zn(II) complexation at pH 7.0 over pH 8.0. This indicates that dehydrating a neutral thiol is more favorable than dehydrating a charged thiolate in this peptide scaffold. In terms of enthalpy, the enthalpy required to break the S−H bonds is more than compensated for by the favorable enthalpic contribution of peptide dehydration. This leads to the less favorable, endothermic reaction enthalpy observed at pH 7.0 relative to pH 8.0. In terms of entropy, water release at pH 7.0 is more favorable by 27 cal K^{-1} mol^{-1}, or −8.0 kcal mol^{-1} at 298 K, than at pH 8.0. This increase in entropy due to water release compensates for the diminished enthalpy required for S−H bond cleavage, yielding a more favorable free energy of reaction.

Although it is difficult to discern the enthalpy and entropy of peptide dehydration in absolute terms, the differences

between pH 7.0 and 8.0 are significant in magnitude. The estimated changes in the entropy of dehydration of the peptide scaffold is three times that of the entropy of water release from Zn(II), estimated to be ~9.5 cal K^{-1} mol^{-1} per water molecule (*62*). Additionally, the change in free energy of water release between these pH values, −15.1 kcal mol^{-1}, is similar in magnitude to the +16 kcal mol^{-1} estimate of the energetic cost to fold a $\beta\beta\alpha$ Cys_2His_2 zinc finger peptide, indicating that the pH dependence of the energetics of peptide dehydration are of sufficient magnitude to compromise protein folding (*47*). Regardless of how one interprets the data, that is, whether the release of protons directly modulates the favorability of the reaction entropy or the protonation state of the *apo*-peptide modulates its dehydration, it is evident that solution pH, often ignored in such analyses, is critical to the coordination chemistry thermodynamics of thiolate rich Zn(II) sites in biology (*63*).

There has been considerable debate in the literature as to the protonation state of cysteine ligands to Zn(II) sites in biology (*56*, *64*, *65*). Computational studies have indicated that $Zn(Cys)_4$ sites may contain at least one thiol ligand at physiological pH values, and mass spectrometry experiments suggest the retention of thiol protons in cysteine rich zinc coordination spheres (*56*, *64*). However, in the case of Zn(II)−**GGG**, the direct determination of the zinc bound cysteine pK_a values, pK_a^{eff}, reveal that the $Zn(Cys)_4$ site is not protonated at physiological pH values but can be protonated at lower pH values. This is indeed the case with other natural cysteine rich zinc binding proteins such as the HIV-1 nucleocapsid protein and the zinc finger of primase, both exhibiting pK_a^{eff} values of ~5.0 (*53*−*55*). The protonated Zn(II)−**GGG**-H^+ complex, K_d^{MLH} value of 19 fM, binds Zn(II) 315-fold weaker than the fully deprotonated complex, Zn(II)−**GGG**. This 315-fold or 3.4 kcal mol^{-1} weaker interaction is due to either the weaker interaction of the protonated thiol ligand with the Zn(II) or its dissociation from Zn(II) and replacement by exogenous water. Further protonation yields the tetra-thiol complex, Zn(II)−**GGG**-$4H^+$, with a K_d^{MLH4} value of 75 μM, which indicates that protonated thiols can have significant affinity for Zn(II). Thus, our findings do not agree with the predictions from computational studies that a proton remains bound to the $Zn(Cys)_4$ site, and they provide an impetus to more accurately parametrize future computational work (*28*−*31*, *56*).

The formation constant of the Zn(II)−**GGG** complex is the tightest measured for a zinc protein to date and may reflect the maximal thermodynamic contribution possible from a Zn(II)−$(S{\cdot}Cys)_4$ site. The limiting K_d^{ML} value of 60 aM is identical, within error, to the corresponding value reported for the Cys_4 site in the related Zn(II)−**IGA** maquette, 125 aM, and slightly tighter than the value reported for the Cys_3His site in the HIV-1 nucleocapsid zinc finger protein, 1.2 fM (*21*, *53*, *54*, *59*). The comparable K_d^{ML} values for Zn(II)−**GGG** and the HIV-1 nucleocapsid protein indicate that the Cys → His change in the primary coordination sphere only weakens the Zn(II) affinity by 20-fold at pH 9.0. The limiting K_d^{ML} for Zn(II)−**GGG** is coincidentally similar to the 1.5 fM value reported for the Zn-sensor protein ZntR, which contains $Zn(S{\cdot}Cys)_3$ and $Zn(S{\cdot}Cys)_2(His)_1$ sites bridged by a phosphate anion. However, their responses to solution pH are quite distinct because of protein folding effects (*51*, *52*). Proton competition attenuates the conditional dissociation constants of Zn(II)−**GGG** below pH 8.3, whereas the K_d value of ZntR is pH independent down to pH 6.5 because of the effect of the protein fold on the *apo*-protein ligand pK_a values. This results in the full realization of the limiting dissociation constant for ZntR at physiological pH, whereas Zn(II)−**GGG** only attains the 60 aM value at pH values above 8.3.

The limiting K_d^{ML} value for Zn(II)−**GGG** represents a −22.1 kcal mol^{-1} free energy contribution to the Zn(II) protein stability, which is an order of magnitude larger than typical protein−protein interactions, that is, hydrogen-bonds and salt bridges. At pH 7.0, where the conditional K_d value is 8.0 pM or −15.1 kcal mol^{-1}, the free energy contribution of the Zn(II)-Cys_4 site remains greater than the global folding free energies of many natural proteins. The magnitude of this interaction demonstrates why Zn(II)-Cys_4 sites can be used to assemble and fold a variety of protein scaffolds (*1*, *57*, *66*−*68*). Furthermore, the demonstration by Woolfson and co-workers that Zn(II) binding four histidine residues can be used to convert a stably folded *apo*-protein into a *holo*-protein with a different fold and oligomerization state, suggests that a Zn(II)-His_4 may possess a comparable free energy, for example, >10 kcal mol^{-1} (*69*).

A comparison of the ΔG^{ML-Obs} values from a series of Zn(II)−$(S{\cdot}Cys)_4$ proteins that undergo metal induced protein folding events provides fresh insight into the role of the metal in the process. The conditional K_d data for Zn(II)−**GGG**, CP-CCCC, and the gene product of BRCA1 L923 indicate that each has picomolar affinity at pH 7.0, which is within the 1.5 kcal mol^{-1} or the 10-fold error of the measurements (*67*, *68*). If the *apo*-ligand pK_a values are near the solution value of cysteine, as expected for unfolded *apo*-proteins, then they each possess similar differences in their thermodynamic barriers to protein folding, that is, $\Delta G_{apo}^{Folding}$ values. Thus, these results indicate that the free energy difference between the *apo*-unfolded and *apo*-folded states in the unstructured 16 amino acid peptide **GGG**, the 26 amino acid $\beta\beta\alpha$ protein CP-CCCC, and the 56 amino acid RING finger domain from the gene product of BRCA 1 are equivalent despite their differences in primary and secondary structure (cf. Scheme 1). Using a structure-based thermodynamic analysis, Blasie and Berg have estimated the $\Delta G_{apo}^{Folding}$ of CP-1, the His_2-Cys_2 prototype of the designed zinc finger protein CP-CCCC, to be +16.0 kcal mol^{-1}, which suggests a ΔG^{ML} value of approximately −38 kcal mol^{-1} for CP-CCCC, Zn(II)−**GGG**, and the RING finger domain (*47*). An alternative interpretation of this result is that there is a minimal free energy difference between the *apo*-unfolded and *apo*-folded states in each of these three proteins. The latter interpretation is supported by several key observations from protein design using the $\beta\beta\alpha$ zinc finger scaffold. First, Imperiali and co-workers have redesigned a zinc finger protein scaffold to stably fold in the absence of metal ion and observe a similar metal-ion affinity as compared to the wild-type protein (*70*). If $\Delta G_{apo}^{Folding}$ was as large as +16 kcal mol^{-1} in the $\beta\beta\alpha$ zinc finger scaffold as suggested by Blasie and Berg, an increase of $>10^{11}$-fold would be expected in the metal-ion affinity because of the preorganization of the metal-ion binding site. Second, Dahiyat and Mayo have used computational redesign to generate a $\beta\beta\alpha$ fold that does not contain a Zn(II) binding site and one that is stably folded in the absence of the metal ion (*6*). This result supports the

Table 2: Entropy−Enthalpy Compensation in Zn(II) Proteins at pH 7.0

	Zn(II)−**GGG** (Cys_4)	HIV-1 nucleocapsid protein (Cys_3His_1)	carbonic anhydrase (His_3OH_1)	CP-1 (Cys_2His_2)
ΔG_{rxn} (kcal mol^{-1})	−15.1[a]	−15.3[b]	−16.4[c]	−15.3[c]
ΔH_{rxn} (kcal mol^{-1})	+6.4[a]	+6.4[b]	−6.3[c]	−21.1[c]
$-T_{298K}\Delta S$ (kcal mol^{-1})	−21.5[a]	−21.7[b]	−10.1[c]	+5.7[c]
ΔS_{rxn} (cal K^{-1} mol^{-1})	+72.0[a]	+72.0[b]	+34.0[c]	−19.0[c]

[a] The values were obtained from this work. [b] The values were obtained from ref 59 (*59*). [c] The values were obtained from ref 47 (*47*).

conclusion that a properly packed hydrophobic core can be more stable than the analogous *holo*-metalloprotein. Third, a Folding@home molecular dynamics simulation result indicates that the unfolded ensemble of a $\beta\beta\alpha$ protein fold corresponds to the native folded state in an average sense, that is, the mean structure hypothesis (*71*). *In toto*, these results suggest that the free energy difference between the *apo*-unfolded and *apo*-folded states of the **GGG**, CP-CCCC, and BRCA1 scaffolds are minimal and that metal-ion binding serves to kinetically template the folding event. Therefore, each possesses the tightest affinity possible for a tetrahedral, tetrathiolate Zn(II) binding site.

Other natural Zn(II) proteins may have larger $\Delta G_{apo}^{Folding}$ values and, therefore, utilize the free energy of metal-ion binding to drive protein folding. One such example is the 37 amino acid XPA zinc finger protein involved in the nucleotide excision repair pathway of DNA repair (*72*). We ascribe the 3.9 kcal mol^{-1} difference between the 158 pM and 200 fM conditional dissociation constant values at pH 7.4 of XPA and Zn(II)−**GGG**, respectively, to the energetic cost to folding the XPA zinc finger transcription factor protein. Thus, in the case of the XPA zinc finger, metal-ion binding thermodynamically drives protein folding by several kcal mol^{-1}.

A comparison of the ITC derived thermodynamics of Zn(II) binding at pH 7.0 between the Cys_4 site in **GGG** and several natural Zn(II) proteins also reveals the presence of enthalpy−entropy compensation (EEC) phenomena as shown in Table 2. EEC is a linear free energy relationship between the enthalpy and entropy of a reaction for a related set of chemical processes, that is, the differences in the change in free energy of a family of chemical processes is small relative to the changes in enthalpy and entropy (*73*). Although there is considerable controversy in the literature concerning whether or not EEC is a real phenomenon or an artifact (*73*−*75*), it is often described as being an intrinsic and ubiquitous property of water (*76*, *77*). Table 2 shows the EEC phenomenon observed for Zn(II) binding to **GGG**, the HIV-1 nucleocapsid protein, CP-1, and carbonic anhydrase, whose free energies of Zn(II) binding are within 1.3 kcal mol^{-1} of each other and within the error of the determinations. A comparison of the value for the Cys_4 site in Zn(II)−**GGG** and the Cys_3His_1 site in the HIV-1 nucleocapsid protein shows that they are virtually identical. This demonstrates that the changes in the primary coordination sphere and protein fold do not significantly alter these specific entropically driven Zn(II) binding events. In the case of the HIV-1 nucleocapsid protein, McLendon and co-workers have argued that the increase in entropy is due to greater configurational entropy in the *holo*-protein than in the *apo* protein (*59*), despite the restraint imposed by ligating to the Zn(II). On the basis of the results of DiTusa and co-workers and the data presented herein, we suggest that a more plausible explanation is that the metal coordination event is driven by water release from both peptide and Zn(II) upon binding (*78*, *79*).

In contrast to these entropically driven Zn(II) binding reactions, ITC data for the designed protein CP-1 shows that Zn(II) binding to the Cys_2His_2 coordination sphere in the $\beta\beta\alpha$ fold is enthalpically favored and entropically disfavored (*47*). Indeed, the reaction enthalpy and entropy values between Zn(II)−**GGG** and CP-1 are almost perfectly reversed, whereas both have comparable Zn(II) affinities at pH 7.0. The reaction enthalpy is +6.4 kcal mol^{-1} unfavorable in Zn(II)−**GGG** and −21.1 kcal mol^{-1} favorable in CP-1; the reaction entropy is −21.5 kcal mol^{-1} favorable in Zn(II)−**GGG** and +5.7 kcal mol^{-1} unfavorable in CP-1. This dramatic enthalpy−entropy compensation, >20 kcal mol^{-1}, reflects several differences between Zn(II)−**GGG** and CP-1. The differences in the coordination sphere contribute to the enthalpy changes, that is, Zn(II)-His versus Zn(II)-Cys bond enthalpy as well as the entropy changes due to changes in the number of protons released upon Zn(II) binding. The greater restriction in protein conformational entropy upon Zn(II) binding to CP-1 relative to Zn(II)−**GGG** is likely a factor in the unfavorable entropy of the former because it is uniquely structured in the *holo*-state. In addition, the hydration of the *apo* and *holo* states of the two scaffolds are likely different and significantly contribute to the observed enthalpy−entropy compensation.

Finally, it is worth comparing the unstructured Zn(II)−**GGG** with a protein that is folded in both the *apo* and *holo* states, carbonic anhydrase. DiTusa and co-workers have shown that incorporation of Zn(II) into the $His_3(OH)_1$ site of carbonic anhydrase is both enthalpically and entropically favored (*78*). Despite the near equivalence in the Zn(II) affinities of Zn(II)−**GGG** and carbonic anhydrase at pH 7.0, Zn(II)−**GGG** is 12.8 kcal mol^{-1} less enthalpically favored and 11.4 kcal mol^{-1} more entropically favored. Although part of the enthalpic difference stems from the differences in His and Cys deprotonation thermodynamics and part of the entropic difference is due to the conformational restriction imposed by Zn(II) binding, it is likely that changes in protein hydration between the *apo* and *holo* states are a significant contributor to the observed EEC.

CONCLUSIONS

In the present work, we demonstrate that a designed protein with minimal structure binds Zn(II) with an affinity greater than the tightest Zn(II)-binding natural proteins. The data illustrate that metalloprotein assembly is entropically driven and that proton release, along with dehydration of both the peptide scaffold and metal ion, exerts considerable influence on the reaction enthalpies, entropies, and free energies. The data from the Zn(II)−**GGG** complex are used to delineate the energetic cost to protein folding in natural proteins with Zn(II)−Cys_4 sites that undergo metal induced protein folding reactions. This comparison demonstrates the

near energetic equivalence of the *apo*-unfolded and *apo*-folded states in some natural zinc finger proteins, with others utilizing part of the free energy of Zn(II) binding to drive protein folding. Additionally, comparison of the thermodynamic parameters for Zn(II) binding by **GGG** to other Cys_x-His_x Zn(II) binding proteins reveals the presence of entropy−enthalpy compensation phenomena at physiological pH and is likely a result of the interplay between peptide and metal dehydration, S−H bond cleavage, and differences in configurational entropy of the protein scaffolds. Our efforts are now focused on evaluating the thermodynamics of Zn(II) binding to Cys_2His_2 and Cys_3His sites relevant to natural zinc finger transcription factors in the same manner as that described herein.

ACKNOWLEDGMENT

We thank Professor Ronald Breslow for the generous use of his Isothermal Titration Calorimeter.

REFERENCES

1. Auld, D. S. (2001) Zinc coordination sphere in biochemical zinc sites, *BioMetals 14*, 271−313.
2. Andreini, C., Banci, L., Bertini, I., and Rosato, A. (2006) Counting the zinc-proteins encoded in the human genome, *J. Proteome Res. 5*, 196−201.
3. Frankel, A. D., Berg, J. M., and Pabo, C. O. (1987) Metal-dependent folding of a single zinc finger from transcription factor IIIA, *Proc. Natl. Acad. Sci. U.S.A. 84*, 4841−4845.
4. Berg, J. M. (1993) Zinc-finger proteins, *Curr. Opin. Struct. Biol. 3*, 11−16.
5. DeGrado, W. F., Summa, C. M., Pavone, V., Nastri, F., and Lombardi, A. (1999) *De novo* design and structural characterization of proteins and metalloproteins, *Annu. Rev. Biochem. 68*, 779−819.
6. Dahiyat, B. I., and Mayo, S. L. (1997) *De novo* protein design: Fully automated sequence selection, *Science 278*, 82−87.
7. Dwyer, M. A., Looger, L. L., and Hellinga, H. W. (2004) Computational design of a biologically active enzyme, *Science 304*, 1967−1971.
8. Kuhlman, B., Dantas, G., Ireton, G. C., Varani, G., Stoddard, B. L., and Baker, D. (2003) Design of a novel globular protein fold with atomic-level accuracy, *Science 302*, 1364−1368.
9. Chin, J. W., and Schepartz, A. (2001) Design and evolution of a miniature Bcl-2 bnding protein, *Angew. Chem., Int. Ed. 40*, 3806−3809.
10. Struthers, M. D., Cheng, R. P., and Imperiali, B. (1996) Design of a monomeric 23-residue polypeptide with defined tertiary structure, *Science 271*, 342−345.
11. Kortemme, T., Ramírez-Alvarado, M., and Serrano, L. (1998) Design of a 20-amino acid, three stranded β-sheet protein, *Science 281*, *253*−*256*.
12. Wilson, C., Apiyo, D., and Wittung-Stafshede, P. (2005) Role of cofactors in metalloprotein folding, *Q. Rev. Biophys. 3*−*4*, 285−314.
13. Ghosh, D., and Pecoraro, V. L. (2005) Probing metal-protein interactions using a de novo design approach, *Curr. Opin. Chem. Biol. 9*, 97−103.
14. Lu, Y. (2005) Design and engineering of metalloproteins containing unnatural amino acids or non-native metal-containing cofactors, *Curr. Opin. Chem. Biol. 9*, 118−126.
15. Robertson, D. E., Farid, R. S., Moser, C. C., Urbauer, J. L., Mulholland, S. E., Pidikiti, R., Lear, J. D., Wand, A. J., DeGrado, W. F., and Dutton, P. L. (1994) Design and synthesis of multihaem proteins, *Nature 368*, 425−432.
16. Reedy, C. J., Kennedy, M. L., and Gibney, B. R. (2003) Thermodynamic characterization of ferric and ferrous haem binding to a designed four-α-helix protein, *Chem. Commun*. 570−571.
17. Petros, A. K., Shaner, S. E., Costello, A. L., Tierney, D. L., and Gibney, B. R. (2004) Comparison of cysteine and penicillamine ligands in a Co(II) maquette, *Inorg. Chem. 43*, 4793−4795.
18. Kennedy, M. L., and Gibney, B. R. (2002) Proton coupling to $[4Fe\text{-}4S]^{2+/+}$ and $[4Fe\text{-}4Se]^{2+/+}$ oxidation/reduction in a designed protein, *J. Am. Chem. Soc. 124*, 6826−6827.
19. Kennedy, M. L., Petros, A. K., and Gibney, B. R. (2004) Cobalt-(II) and zinc(II) binding to a ferredoxin maquette, *J. Inorg. Biochem. 98*, 727−732.
20. Gibney, B. R., Mulholland, S. E., Rabanal, F., and Dutton, P. L. (1996) Ferredoxin and ferredoxin-heme maquettes, *Proc. Natl. Acad. Sci., U.S.A. 93*, 15041−15046.
21. Petros, A. K., Reddi, A. R., Kennedy, M. L., Hyslop, A. G., and Gibney, B. R. (2006) Femtomolar Zn(II) affinity in a peptide ligand designed to model thiolate-rich metalloprotein active sites, *Inorg. Chem. 45*, 9941−9958.
22. Privett, H. K., Reedy, C. J., Kennedy, M. L., and Gibney, B. R. (2002) Nonnatural amino acid ligands in heme protein design, *J. Am. Chem. Soc. 124*, 6828−6829.
23. Zhuang, J., Amoroso, J. H., Kinloch, R., Dawson, J. H., Baldwin, M. J., and Gibney, B. R. (2004) Design of a five-coordinate heme protein maquette: A spectroscopic model of deoxy myoglobin, *Inorg. Chem. 43*, 8218−8220.
24. Zhuang, J., Amoroso, J. H., Kinloch, R., Dawson, J. H., Baldwin, M. J., and Gibney, B. R. (2006) Evaluation of electron-withdrawing group effects on heme binding in designed proteins: Implications for heme a in cytochrome c oxidase, *Inorg. Chem. 45*, 4685−4694.
25. Zhuang, J., Reddi, A. R., Wang, Z., Khodaverdian, B., Hegg, E. L., and Gibney, B. R. (2006) Evaluating the roles of the heme a sidechains in cytochrome c oxidase using designed heme proteins, *Biochemistry 45*, 12530−12538.
26. Reddi, A. R., Reedy, C. J., Mui, S., and Gibney, B. R. (2007) Thermodynamic investigation into the mechanisms of proton-coupled electron transfer events in heme-protein maquettes, *Biochemistry 46*, 291−305.
27. Hong, J., Kharenko, O., Fan, J., Xie, F., Petros, A. K., Gibney, B. R., and Ogawa, M. Y. (2006) Evidence that a miniature Cu(I) metalloprotein undergoes collisional electron transfer in the Marcus inverted region, *Angew. Chem., Int. Ed. 45*, 6137−6140.
28. Schymkowitz, J. W. H., Rousseau, F., Martins, I. C., Ferkinghoff-Borg, J., Stricher, F., and Serrano, L. (2005) Prediction of water and metal binding sites and their affinities by using the Fold-X force field. *Proc. Natl. Acad. Sci. U.S.A. 102*, 10147−10152.
29. Dudev, T., and Lim, C. (2001) Modeling Zn^{2+}-cysteinate complexes in proteins, *J. Phys. Chem. B 105*, 10709−10714.
30. Calimet, N., and Simonson, T. (2006) Cys_xHis_y-Zn^{2+} interactions: Possibilities and limitations of a simple pairwise force field, *J. Mol. Graphics Modell. 24*, 404−411.
31. Dudev, T., and Lim, C. (2003) Principles governing Mg, Ca, and Zn binding and selectivity in proteins, *Chem. Rev. 103*, 773−787.
32. Christian, L., Piotrowiak, P., and Farid, R. S. (2003) Mimicking photosynthesis in a computationally designed synthetic metalloprotein, *J. Am. Chem. Soc. 125*, 11814−11815.
33. Calhoun, J. R., Kono, H., Lahr, S., Wang, W., DeGrado, W. F., and Saven, J. G. (2003) Computational design and characterization of a monomeric helical dinuclear metalloprotein, *J. Mol. Biol. 334*, 1101−1115.
34. Kornilova, A. Y., Wishart, J. F., Xiao, W., Lasey, R. C., Federova, A., Shin, Y-K., and Ogawa, M. Y. (2000) Design and characterization of a synthetic electron-transfer protein, *J. Am. Chem. Soc. 122*, 7999−8006.
35. Benson, D. E., Wisz, M. S., and Hellinga, H. W. (1998) The development of new biotechnologies using metalloprotein design. *Curr. Opin. Biotechnol. 9*, 370−376.
36. Kennedy, M. L., and Gibney, B. R. (2001) Metalloprotein and redox protein design, *Curr. Opin. Sruct. Biol. 11*, 485−90.
37. Kates, S. A., and Albericio, F. (2000) *Solid-Phase Synthesis: A Practical Guide*, Marcel Dekker, New York.
38. Martell, A. E., and Smith, R. M. (1974) *Critical Stability Constants*, Vol. 1, Plenum Press, New York.
39. Wiseman, T., Williston, S., Brandts, J. F., and Lin, L. N. (1989) Rapid measurement of binding constants and heats of binding using a new titration calorimeter, *Anal. Biochem. 179*, 131−137.
40. Freire, E., Mayorga, O., and Straume, M. (1990) Isothermal titration calorimetry, *Anal. Biochem. 62*, 950A-959A.
41. Ladbury, J. E., and Chowdhry, B. Z. (1996) Sensing the heat: the application of isothermal titration calorimetry to thermodynamic studies of biomolecular interactions, *Chem. Biol. 3*, 791−801.

42. Zhang, Y., Akilesh, S., and Wilcox, D. E. (2000) Isothermal titration calorimetry measurements of Ni(II) and Cu(II) binding to His, GlyGlyHis, HisGlyHis and bovine serum albumin: a critical evaluation, *Inorg. Chem. 39*, 3057−3064.
43. Richens, D. T. (1997) *The Chemistry of Aqua Ions*, John Wiley & Sons, New York.
44. Zhu, M., and Pan, G. (2005) Quantum chemical studies of mononuclear zinc species of hydration and hydrolysis, *J. Phys. Chem. A 109*, 7648−7652.
45. Fukada, H., and Takahashi, K. (1998) Enthalpy and heat capacity changes for the proton dissociation of various buffer components in 0.1 M potassium chloride, *Proteins 33*, 159−166.
46. Pavletich, N. P., and Pabo, C. O. (1991) Zinc finger-DNA recognition: Crystal structure of a Zif268-DNA complex at 2.1 Å, *Science 252*, 809−817.
47. Blaise, C. A., and Berg, J. M. (2002) Structure-based thermodynamic analysis of a coupled metal binding-protein folding reaction involving a zinc finger peptide, *Biochemistry 41*, 15068−15073.
48. Magyar, J. S., and Godwin, H. A. (2003) Spectropotentiometric analysis of metal binding to structural zinc-binding sites: accounting quantitatively for pH and metal ion buffering effects, *Anal. Biochem. 320*, 39−54.
49. Harris, H. L., and Hudson, B. S. (1990) Photophysics of tryptophan in bacteriophage T4 lysozymes, *Biochemistry 29*, 5276−5285.
50. Lakshmikanth, G. S., and Krishnamoorthy, G. (1999) Solvent-exposed tryptophans probe the dynamics at protein surfaces, *Biophys. J. 77*, 1100−1106.
51. Hitomi, Y., Outten, C. E., and O'Halloran, T. V. (2001) Extreme zinc-binding thermodynamics of the metal sensor/regulator protein, ZntR, *J. Am. Chem. Soc. 123*, 8614−8615.
52. Outten, C. E., and O'Halloran, T. V. (2001) Femtomolar sensitivity of metalloregulatory proteins controlling zinc homeostasis, *Science 292*, 2488−2492.
53. Bombarda, E., Cherradi, H., Morellet, N., Roques, B. P., and Mély, Y. (2002) Zn^{2+} binding properties of single-point mutants of the C-terminal zinc finger of the HIV-1 nucleocapsid protein: Evidence of a critical role of cysteine 49 in Zn^{2+} dissociation, *Biochemistry 41*, 4312−4320.
54. Bombarda, E., Morellet, N., Cherradi, H., Spiess, B., Bouaziz, S., Grell, E., Roques, B. P., and Mély, Y. (2001) Determination of the pK_a of the four Zn^{2+}-coordinating residues of the distal finger motif of the HIV-1 nucleocapsid protein: Consequences of the binding of Zn^{2+}, *J. Mol. Biol. 310*, 659−672.
55. Griep, M. A., Adkins, B. J., Hromas, D., Johnson, S., and Miller, J. (1997) The tyrosine photophysics of a primase-derived are sensitive to the peptide's zinc-bound state: Proof that the bacterial primase hypothetical zinc finger sequence binds zinc, *Biochemistry 36*, 544−553.
56. Simonson, T., and Calimet, N. (2002) Cys_xHis_y-Zn^{2+} interactions: Thiol vs. thiolate coordination, *Proteins 49*, 37−48.
57. Payne, J. C., Rous, B. W., Tenderholt, A. L., and Godwin, H. A. (2003) Spectroscopic determination of the binding affinity of zinc to the DNA-binding domains of nuclear hormone receptors, *Biochemistry 42*, 14214−14224.
58. Gladysheva, T., Liu, J., and Rosen, B. P. (1996) His-8 lowers the pK_a of the essential Cys-12 residue of the ArsC arsenate reductase of plasmid R773, *J. Biol. Chem. 271*, 33256−33260.
59. McLendon, G., Hull, H., and Larkin, K., and Chang, W. (1999) Metal binding to the HIV nucleocapsid peptide, *J. Biol. Inorg. Chem. 4*, 171−174.
60. Bryson, J. W., Betz, S. F., Lu, H. S., Suich, D. J., Zhou, H. X., O'Neil, K. T., and DeGrado, W. F. (1995) Protein design: a hierarchic approach, *Science 270*, 935−941.
61. Wrathall, D. P., Izatt, R. M., and Christensen, J. J. (1964) Thermodynamics of proton dissociation in aqueous solution. III. L-cysteine, L-methyl-L-cysteine, and mercaptoacetic acid. Determination of cysteine microconstants from calorimetric data, *J. Am. Chem. Soc. 86*, 4779−478359.
62. Dunitz, J. D. (1994) The entropic cost of bound water in crystals and biomolecules, *Science 264*, 670.
63. Lachenmann, M. J., Ladbury, J. E., Dong, J., Huang, K., Carey, P., and Weiss, M. A. (2004) Why zinc fingers prefer zinc: Ligand-field symmetry and hidden thermodynamics of metal ion selectivity, *Biochemistry 43*, 13910−13925.
64. Fabris, D., Zaia, J., Hathout, Y., and Fenselau, C. (1996) Retention of thiol protons in two classes of protein zinc ion coordination centers, *J. Am. Chem. Soc. 118*, 12242−12243.
65. Sousa, S. F., Fernandes, P. A., and Ramos, M. J. (2005) Farnesyltransferase: Theoretical studies on peptide substrate entrance: thiol or thiolate coordination? *J. Mol. Struct. 729*, 125−129.
66. Berg, J. M. (1995) Zinc finger domains: From predictions to design, *Acc. Chem. Res. 28*, 14−19.
67. Krizek, B. A., Merkle, D. L., and Berg, J. M. (1993) Ligand variation and metal ion binding specificity in zinc finger peptides, *Inorg. Chem. 32*, 937−940.
68. Roehm, P. C., and Berg, J. M. (1997) Sequential metal binding by the RING finger domain of BRCA 1, *Biochemistry 36*, 10240−10245.
69. Cerasoli, E., Sharpe, B. K., and Woolfson, D. N. (2005) ZiCo: A peptide designed to switch folded state upon binding zinc, *J. Am. Chem. Soc. 127*, 15008−15009.
70. Struthers, M. D., Cheng, R. P., and Imperiali, B. (1996) Economy in protein design: Evolution of a metal-independent $\beta\beta\alpha$ motif based on the zinc finger domains, *J. Am. Chem. Soc. 118*, 3073−3081.
71. Zagrovic, B., Snow, C. D., Khaliq, S., Shirts, M. R., and Pande, V. S. (2002) Native-like mean structure in the unfolded ensemble of small proteins, *J. Mol. Biol. 323*, 153−164.
72. Bal, W., Schwerdtle, T., and Hartwig, A. (2003) Mechanism of nickel assault on the zinc finger of DNA repair protein XPA, *Chem. Res. Toxicol. 16*, 242−248.
73. Sharp, K. (2001) Entropy-enthalpy compensation: Fact or artifact, *Protein Sci. 10*, 661−667.
74. Beasley, J. R., Doyle, D. F., Chen, L., Cohen, D. S., Fine, B. R., and Pielak, G. J. (2002) Searching for a quantitative entropy-enthalpy compensation among protein variants, *Proteins 49*, 398−402.
75. Liu, L., and Guo, Q.-X. (2001) Isokinetic relationship, isoequilibrium relationship, and enthalpy-entropy compensation, *Chem. Rev. 101*, 673−696.
76. Lumry, R., and Rajender, S. (1970) Enthalpy-entropy compensation phenomena in water solutions of proteins and small molecules: A ubiquitous property of water, *Biopolymers 9*, 1125−1227.
77. Blasie, C. A., and Berg, J. M. (2004) Entropy-enthalpy compensation in ionic interactions probed in a zinc finger peptide, *Biochemistry 43*, 10600−10604.
78. DiTusa, C. A., Christensen, T., McCall, K. A., Fierke, C. A., and Toone, E. J. (2001) Thermodynamics of metal ion binding. 1. Metal ion binding by wild type carbonic anhydrase, *Biochemistry 40*, 5338−5344.
79. DiTusa, C. A., McCall, K. A., Christensen, T., Mahapatro, M., Fierke, C. A., and Toone, E. J. (2001) Thermodynamics of metal ion binding. 2. Metal ion binding by carbonic anhydrase variants, *Biochemistry 40*, 5345−5351.

BI062253W